An Algorithm for Seam Tracking Applications

P. K. Khosla, C. P. Neuman, and F. B. Prinz

CMU-RI-TR-84-6

The Robotics Institute
Carnegie-Mellon University
Pittsburgh, Pennsylvania 15213

May 1984

This work has been supported by the Inlaks Foundation, U. K., and the Department of Electrical and Computer Engineering and Welding Consortium, Robotics Institute, Carnegie-Mellon University.

Table of Contents

List of Figures

List of Tables

Abstract

Seam tracking is currently accomplished by special features of the robot and *a priori* knowledge of seam geometry. In this paper we demonstrate the feasibility of tracking a seam in real-time. A general-purpose seam tracking algorithm is developed for implementation on a robot with six degrees-of-freedom. The algorithm is motivated by a physical interpretation of the T_6 and dT_6 matrices, and the assumption that 3-D seam data are available. In the past, the dTV matrix and inverse Jacobian solutions have been used to compute the differential changes in the joint angles. By using the inverse Jacobian, an iterative algorithm is introduced to compute both large and small changes in the joint variables. The versatile seam tracking algorithm can be applied to a multitude of robotic seam tracking activities such as gluing, surface grinding and flame cutting.

1. Introduction

Manufacturing operations such as robotic welding, gluing, sealing and surface grinding require trajectory control of the tool mounted on the end-effector of the robot. While the kinematic control algorithm developed in this paper is applicable to a multitude of manufacturing operations, robotic arc welding nomenclature is used. The tool is called the welding torch, and the tool trajectory is defined by the weld scam. The fundamental problem is to position a welding gun with the proper translational and rotational positions with respect to a curved weld scam in three dimensional (3-D) space. A scam in space can be traced by a five degrcc-of-freedom robot. Since real-time seam tracing requires that *both* the sensor *and* torch trace the seam, a six degrcc-of-freedom robot is required. Automation of the welding process thus demands a robot with *six* degrces-of-freedom and acceptable performance in terms of speed and accuracy. The control task also demands a *real-time* algorithm to guide the robot in a fixed geometrical relationship to die contour.

Automation of the welding process can be divided into two distinct components :

- Scam data acquisition and interpretation by a sensor system ; and
- Guidance* and control of the robot to traverse the seam, while maintaining the proper orientation and position.

Since the scam data constitute the 3-D coordinates of the seam, a visual sensory device (such as a light stripe imaging device) can be used to obtain the seam data. Methods for obtaining 3-D data from 2-D images have been developed [Agin 82]. Having obtained and interpreted the scam data, the control system must guide die robot to traverse the scam and place the requisite amount of weld material along the path. The torch position and attitude must be controlled precisely to ensure acceptable weld quality.

Scam tracking is currently accomplished by exploiting a special feature of the robot or limiting the application to a particular type of a seam. Bollingcr and Harrison [Bollinger 71] describe the principles and techniques of a spatial scam tracking system. In this application, the seam is constrained to lie on a cylindrical surface. Tomi/.uka, *et ah* [Tomizuka 80] propose a preview control strategy for two-axis welding torch positioning and velocity control. The scheme is only applicable for two-axis control and hence constrains the scam to lie in a plane. Furthermore, the scheme cannot be implemented on a general purpose six degrcc-of-frccdom robot.

One of the first successful demonstrations of computer vision to arc welding is the NASA *weld skate [HWl* 80]. This system has been implemented on a special-purpose robot and requires special edge preparation to operate properly. The system is incapable of making any determination regarding the joint fit-up. The principle of structured illumination has been employed by Kawasaki Heavy Industries of Japan [Masaki 79] to develop a visual seam tracking system. The approach used for image analysis is *training-by-showiug.* A set of typical images is acquired in a teaching operation prior to welding and stored in the memory of the processor. As real-time images are acquired, a search is conducted (through the set of trained images) until a match is found. During the matching process, the positional displacement between the two images is computed and used to correct the position of the torch. The system has been designed specifically for the ship building industry and hence operates only on fillet joints. The system does not utilize part fit-up information for seam tracking.

An example of wclding-by-tcaching is the system described by Masaki, *et al* [Masaki 81] which has a visual scam tracking capability. The robot is taught the reference path for the end-effector and the reference image for the image processor. In the teach mode, two passes arc required for each work piece, one for sensing and one for welding. The path for the welding operation is generated from the sensing pass information.

Current robot welding systems are thus suitable for large batches of parts which are cut and fit to tight tolerances. The robot must trace and weld a scam, within acceptable tolerance limits, on such closely fit parts. Another limiting factor for a semi-automated welding system is the robot programming and set-up time in the shop when the part is changed. These constraints may be eased through the introduction of a CAD/CAM data base in which tlie welding trajectories and speed, weave pattern, wire feed rate, voltage and current are stored for each welding part and then retrieved as required. Unpredictable fit-up and loose part tolerances create the need for a real-time guidance and control algorithm.

The objective of this paper is to introduce a versatile scam tracing algorithm that demonstrates the feasibility of tracking a scam in real-time. The general purpose seam tracing algorithm can be implcmcntablcd on any robot with six degrccs-of-freedom. The algorithm is motivated by the physical interpretation of tlie forward solution, or T_6 matrix [Paul 81] and tlie inverse Jacobian. To facilitate implementation of the inverse Jacobian solutions, an iterative algorithm is developed to compute the differential changes in the joint variables from tlie dT_6 matrix. To reduce significantly the on-line computational requirements, the concept of a modified dT_6 matrix is also introduced. To evaluate the performance of the scam tracing algorithm, a functional simulation package (for the Cyro[1] robot in our laboratory) has been implemented. The outputs of tlie simulation arc the joint position and velocity set-points for tlie robot control system.

The paper is organized as follows. The kinematics of the Cyro robot (including the forward and reverse solutions , and the Jacobian and inverse Jacobian) are developed in Section 2. The foundations for the scam tracking algorithm are laid in Section 3. Focus is on the specification of the T_6 matrices at tlie sample points

[1] **Cyro is a trademark of the Advanced Robotics Corporation.**

along the seam and planning the motion of the torch. To reduce the computational requirements of the algorithm for real-time applications, the concept of the modified dT_6 matrix is introduced in Section 4, and an iterative algorithm to compute both large and small changes in the joint coordinates is then developed. The computational requirements arc enumerated to indicate the potential for die real-time implementation of the algorithm. The salient features of the simulator, which has been implemented to evaluate the performance of the scam tracing algorithm, arc presented in Section 5. Simulation experiments for representative test cases are then highlighted in Section 6. Finally, in Section 7, conclusions arc drawn from the simulation experiments, and the paper is summarized.

2. Kinematics of the Cyro Robot

The forward solution (or T_6 matrix) of die robot, from the base frame to the torch (or end-effector) frame, is developed using homogeneous transformations [Paul 81]. The homogeneous transformations, relating two successive coordinate frames, are only a function of the six joint coordinates. Thus, knowledge of all of the six joint coordinates leads to the transformation (or forward solution) from the base frame to the torch frame.

To develop the homogeneous transformation or A matrices, a coordinate frame is embedded in each of the six links of the robot, using the Dcnavit-Hartcnbcrg convention [Dcnavit 55]. The coordinate frames are shown in Figure 1. Joints 1;* 2 and 6 are rcvolute, and joints 3, 4 and 5 are prismatic. The coordinates of the rcvolute joints arc $\#_1$, $\$_2$ and $0'_6$, and the coordinates of the prismatic joints are $x\sim_3$ z_4 and yy_5. The subscripts on the coordinates indicate the joint number; the base is link zero. The base coordinate frame is fixed at the center of the table of the robot and coincides with the first coordinate frame. When *all* of the six joint coordinates arc zero, the axes for joint 1 (table) and joint 6 (torch) arc parallel and the robot becomes singular. In the algorithm, the manipulator is assumed to be at the zero position. Without loss of generality, the constant offsets of die robot are assumed to be zero. A counter-clockwise rotation of the revolute joints is considered to be positive,, and translation of die prismatic joints along the positive z-axis is considered to be positive.

The link parameters of the Cyro robot arc listed in Table 1, and the forward solution is displayed in Table 2. Having obtained the forward solution, the values of the joint coordinates that led to the $1"_6$ matrix can be computed. This reverse solution [Paul 81] is required (by the simulator) to relate the T_6 matrix to the present values of the joint coordinates. The reverse solution is listed in Table 3.

The differential changes in the cartesian coordinates of the torch are related to the differential changes in the joint coordinates through the manipulator Jacobian [Whitney 72, Paul 81]. Each column of the Jacobian matrix J is a differential translation and rotation vector. The column vectors of

$$J = \begin{bmatrix} \frac{\partial T_6}{\partial \theta_1} & \frac{9T_6}{9\#2} & \frac{9T_6}{9\wedge 3} & \frac{9T_6}{9z_4} & \frac{9T_6}{9y_5} & \frac{9T_6}{9\#_6} \end{bmatrix}$$

arc listed in Table 4.

In scam tracing, sensory data can be utilized to determine the incremental change in the position of die seam from differential changes in the elements of the T_{fi} matrix. The differential change matrix dT_6 is thus available tri plan the incremental motions of the torch. It thus becomes imperative to find the inverse Jacobian (or incremental changes in the joint coordinates) which produce the specified incremental change in the $T,_0$ matrix.

Numerical inversion of die Jacobian [Whitney 72] is computationally intensive and hence is not suitable for real-time control applications. Incremental changes in the joint coordinates can be obtained from a Taylor scries expansion of the reverse solution. Such an approach leads to analytical formulae for the differential joint coordinates which are functions of the elements of the T_6 and dT_6 matrices [Paul 81]. Analytical formulae for the differential joint coordinates, which arc obtained by differentiating the reverse solution (in Table 3), are listed in Table 5.

3. Kinematic Seam Tracking Control

The control task is to fill a volume with weld material while maintaining the proper position and orientation of the torch with respect to the seam. While traversing the seam, the tip of the torch traces a curve in 3-D space. If the discrete points on the curve to be traced and the surface containing the curve arc identified, the T_6 matrices can be generated for each point on the discrctized curve.

Specification of the T_6 matrices at the sample points of the discretized curve accomplishes die seam tracing task. The T_{A_0} matrix is

$$'T_6 = \begin{bmatrix} n & o & a & p \\ 0 & 0 & 0 & 1 \end{bmatrix} = \begin{bmatrix} n_x & o_x & a_x & p_x \\ n_y & {}^{o}y & a_y & Py \\ n_z & o_{7.} & a_{7.} & P/. \\ 0 & 0 & 0 & 1 \end{bmatrix}$$

and represents the position and orientation of the torch shown in Figure 2. The origin of the describing coordinate frame is located at the tip of the torch and is described by the vector p with respect to the base frame. The three unit vectors n, o and a, which describe the orientation relative to the base frame, are directed as follows [Paul 81]. The z-axis of the describing frame lies along the direction that the torch approaches die surface (containing the curve to be traced) and is called the approach vector a. The y-axis of the describing frame lies along the direction of the boom holding the camera and is called die orientation vector o. The normal vector n is then chosen to form a right-handed set of vectors and is computed as

ťt = 3 x 3

The vectors n, o and a describing the orientation of the torch and the vector p describing the position can be specified independently. The control task can thus be split into two independent components :

- Tracing a curve in 3-D space; and
- Maintaining proper orientation of the torch with respect to die surface which contains the curve to be traced.

The volume to be filled with the weld material is contained within two surfaces (of metal) which arc to be joined together. The surfaces may be non-overlapping, as in the case of a butt joint (in Figure 3), or overlapping as in the case of a lap joint or a fillet joint.

Let *m* be a curve (in 3-D space) which lies on the surface *S* and is to be tiaccd by the tip of the torch. The surface *S* may have a varying slope. Henceforth, the curve *m* will be termed the *mid-seam*. The mid-scam is discrcti/cd length-wise. Let nr$_i$ be the vector (with respect to the base frame) pointing to the i-th sample point m$_i$ on the mid-scam. The discretization is specified to allow a picccwisc linear approximation of the curve *m* between two adjacent sample points. If the surface (in the vicinity of the two sample points tn.$_i$ and m.$_{i+i}$) is also discrctized, then a pieccwisc planar approximation of *S* is obtained. Let *P*$_i$ denote the plane (containing the points m$_i$ and m$_{i+}$ j). The direction cosines of the plane specify the orientation of the torch which is held constant for the duration of travel from m.$_i$ to m$_{i+i}$.

The position of the torch is specified by the coordinates of the sample points. The foregoing description of the position and the orientation of the torch completes the formulation of the T_6 matrix at die sample points. The ensuing section specifics the T_6 matrix for butt, lap and fillet joints.

3.1. Specification of the T_6 Matrix

Having interpreted physically the elements of the T_6 matrix, die next step is to generate numerical values of the elements of the T_6 matrix in terms of the coordinates of the sample points obtained from the sensor system. Since a light stripe projector and a solid state camera are assumed to be used as the sensory device, the 3-D coordinates of the points on the surfaces to be joined arc mapped into pixels in the camera image. Figure 4 shows a typical camera image (at the i-th sampling instant) obtained from a butt joint. The break points in the camera images of the surface indicate the discontinuity in *the* actual surfaces to be welded. To specify the curve to be traced, it is essential to extract 3-D coordinates of the break points in the images. The information regarding the orientation of the surfaces, in the vicinity of the break points, can be obtained by extracting the coordinates of one additional point on each surface. The break points are called $u_{.1}$ and v_i for the butt joint shown in Figure 3. The additional points on each of the two surfaces arc called p_t and $q.$^ respectively. The subscript i denotes the sampling instant. The coordinates of the sample points are specified with respect to the base frame of the robot, and $p_{.i}$, $u_{.i}$, v_i and q_i arc die vectors from the origin of the base frame to the points p_p $u_{.,i}$ $v_{.i}$ and $q_{\{}$ respectively. The edges formed by die sample points { $p_{.i}$ }, { $q_{.\{}$ }, { $u_{.1}$ } and { $v_{.i}$ } arc denoted by /?, r/, M, and v, respectively.

To specify the p vector of the T_6 matrix requires knowledge of the sample points along the mid-scam. For a butt joint, the requirement that the torch be placed exactly in the middle across the *u* and v edges forces the x, y and z coordinates of the mid-seam to be computed as:

$$m_{xi} = \frac{u_{xi} + v_{xi}}{2}$$
$$m_{yi} = \frac{u_{yi} + v_{yi}}{2}$$
$$m_{II}\cdot = \frac{u_{zi} + v_{zi}}{2}$$

0)

For both lap and fillet joints, torch stand-off is an important consideration for obtaining a quality weld. Let the desired torch stand-off be characterized by the parameter s, where s ranges from 0 to 1. The coordinates of the mid-seam are then computed as

$$m_{xi} = u_{xi} + s(v_{xi} - u_{xi})$$
$$m_{yi} = u_{yi} + s(v_{yi} - u_{yi})$$
$$m_{zi} = u_{zi} + s(v_{zi} - u_{zi})$$

(2)

The p_x, p_y and p_z components of the T_6 matrix are

$$P_x = m_{xi}$$ ^3>

$$p_z = m_{zi}$$ (ɔ)

and specify completely the last column of the T_6 matrix.

Practical seams have edges with slowly-varying slopes. Since the sample points are assumed to lie close to each other (typically separated by 1 mm), the edges between two sample points can be approximated by a straight line. This approximation leads to a planc which Passes thl0llSh at least ^ircc of the four sample points (Pi, p_{i}.+,, q_{i}., $q_{i+\{}$). The direction cosir. *CS of ^ planc arc also thc direction cosi»cs of a vector normal to the plane. Since'the torch is required to be \DC1Pcndicular "> the *fictitious* scam surface, thc direction cosines of thc approach vector a are specified as th'° *negalive* of thc dircction cosincs * ^ normal to thc plane.

Thc values of thc components of thc orientation vector o ^ computcd under ^ following constraint. When thc torch and the camera arc on thc seam, both should trac k tho SCam, This condition guarantees that sample points will not be lost if the slope of thc mid-edge (at thc poi'nt ofthC torch) dlffcrs from thc slope at thc point-of-vicw of thc camera. Let M be a constant shift in thc numbc."ofsamP|c P()i«ts between thc torch and thc camera. Figure 2 shows that the o vector is perpendicular to tl.>e a vcctor and points along thc direction of the arm holding the camera. If thc camera is traveling in the direction o* L,1C line joining in_{i+N-1} and m_{i+N}, then tlic robot system will never lose track of the scam, unless thc slope experiences large changes or discontinuities along thc scam.

The equation of a plane passing through three of thc four points (p_{i+1V} Pj_{+1}\-v Q_{+} *w* ^i + N-l^ can now ^e specified, and **tlic** angle between thc planes at thc camera and the torch points can be determined. If *(X_v* /x_r *$v_{\{}$)* and (X_2, ju_2, *vj* arc thc dircction cosincs of thc two planes, then thc cosine of angle *0* between thc planes is

$$\cos(0) = XiA2 + /MM2 + \wedge 1 \wedge 2 \tag{6}$$

Thc vector a joining the points ni_{j+N-1} and m_{i+N} along thc mid-edge is computed as

$$\vec{a} = \vec{m}_{i+N} - \vec{m}_{i+N-1} \tag{7}$$

The projection of the vector a onto thc torch plane is chosen to be the o vector and is normalized to be of unit length. Having obtained the normalized o and a vectors, tlic n vector is computed as

$$a = 3 \times 3 \tag{8}$$

to specify completely the T_6 matrix at the sample points.

While traversing from the i-th to the (i-f-l)-th point, die orientation of thc torch and consequently tlic n, o and a vectors remain constant. The p vector in the T_6 matrix changes linearly because of thc straight line approximation between the two points. To maintain a continuous speed and acceleration at **tlic** end points of the segment, the motion of the torch is planned.

3.2. Planning the Motion of the Torch

ThP mnrinn of the tio of thc torch, in traversing a scgr; # I ne motion 01 me up ui {Qn^ |S composcc| of two parts:

- Motion along the segment, and
- Transition between segments.

To make a smooth transition bctwo ^ scgmcnts< jt js desirable to maintain a continuous velocity and acceleration at the transition points. To spccify thc transition equations, a fourth-order curve is fit between the point where a transition star'tS-"an(j ^Q pojnt jnc|jcaljng thc end of thc transition [Paul 81]. The equations for thc transition trajcctorics> ancj velocities arc outlined in Section 3.3.

Let M be thc totorf number of transition steps in which thc desired change in T_6 is to occur. The differential changes in the $v_t(o$ and a vectors at each transition point are

$$\Delta\vec{n} = \frac{\vec{n}_{(i+1)} - \vec{n}_i}{M} \tag{9}$$

$$A! = \frac{\vec{a}_{(i+1)} - \vec{a}_i}{M} \tag{10}$$

$$A3 = \frac{\vec{o}_{(i+1)} - \vec{o}_i}{M} \tag{11}$$

where the subscripts i and (i + 1) denote the i-th and (i + l)-th segments, respectively. 'Hie An, Ao and Aa vectors arc then added to die current n, o and a vectors, respectively, and normalized to unit length, to produce thc n, o and a vectors at the next segment. Let n_p, o_p, a_p and n_n, o_n, a_n be thc vectors of the T_6 matrix at thc present and next segments, respectively; and let thc subscript N indicate that these vectors have been normalized to unit length. The n_u, o_n and a_n vectors arc thus computed as follows :

$$fin =(rtp +\vec{An})_N \tag{12}$$

$$\vec{o}_n = (\vec{o}_p + \vec{\Delta o})_N \tag{13}$$

$$\vec{a}_n = (\vec{a}_p + \vec{A}a)_N \tag{14}$$

Having computed the three component vectors (n, o and a) of T_6 at the next segment, the first three columns of the differential change matrix dT_6 are determined, and the fourth column (or dp vector) can be computed from the transition trajectory to specify the differential translation. The differential change matrix dT_6 is then

$$dT_6 = \begin{bmatrix} dn_x & do_x & da_x & dp_x \\ dn_y & do_y & da_y & dp_y \\ dn_z & do_z & da_7 & dp, \\ 0 & 0 & 0 & 0 \end{bmatrix} \tag{15}$$

where the differential vector components (dn, do, da and dp) of the dT_6 matrix represent the corresponding change in the vector components (n, o, a and p) of the T_6 matrix.

Having generated the present T_6 matrix and d'l $_6$ matrix to reach the next point, the inverse Jacobian (in Table 5) is used to compute *iterative!)'* the differential changes in the joint coordinates. 'The inverse Jacobian solutions arc derived under the assumption that the changes in the joint variables leading to the specified dT_6 matrix are *small.* To overcome the practical fact that this assumption is *not* always satisfied in scam tracing applications, an iterative technique is developed to compute the changes in the joint variables. The velocity set-points during the transition are obtained by dividing the incremental values of the joint variables by the time required to make the incremental change. The transition ends when the torch reaches the point D on the segment B-C in Figure 5. At this point, the torch has the required orientation and velocity to track the (i + l)-di segment I>C without error. This motion is called *motion-along-the-segment.*

During the motion of the torch, along the segment, the n, o and a vectors of the-robot remain constant. The updated dT_6 matrix is specified as:

$$<n'6= \begin{bmatrix} 0 & 0 & 0 & dp_x \\ 0 & 0 & 0 & dp_y \\ 0 & 0 & 0 & dp_z \\ 0 & 0 & 0 & 0 \end{bmatrix} \tag{16}$$

where d p.. dp_v and dp., arc the differential changes in the x, y and z coordinates of the (i + l)-th transition point. When the torch reaches the next transition point, the process of planning the motion of the torch, along the segment and during the transition, is repeated to plan the motion for the next segment.

3.3. The Transition Curves

A transition segment is illustrated in Figure 5. The transition starts at point A in the i-th segment and ends at point D in the (i-f l)-th segment. Maintaining a continuous velocity and acceleration at the points A and D appears to require that six boundary conditions be satisfied. A fifth-order polynomial (with six parameters) would then be needed to approximate the cartesian transition curve. *Symmetry* of the transition guarantees that a *quartic* polynomial can approximate the cartesian transition curve [Paul 81|[2]. To facilitate the development, let T be the transition time and T be the time required to traverse the segment ft-C. The time of travci (T) across a segment is computed by dividing the volume of the weld material (to be deposited along the segment) by the weld-wire volumetric feed-rate, which is assumed to be constant. 'The ratio (r/T) is specified by the engineer (in Section 6). Let the *normalized* time-step parameter h be defined according to

$$h = \frac{t + \tau}{2T} \tag{17}$$

where t denotes the running time-variable (-T < t < T).

Let the fourth-order polynomial approximating the cartesian transition segment be

$$X(h) = \beta_4 h^4 + \beta_3 h^3 + \beta_2 h^2 + \beta_1 h + \beta_0$$

where the five parameters (*fi*$_i$ for i = 0 to 4) must be selected for X(h) to satisfy the boundary conditions [Paul 81]:

$$X(0) = A \;; \qquad X(l) = (C-B)\hat{\ }_{\iota} r + B$$

(18)

$$\dot{X}(0) = 2(B-A) \;; \qquad \dot{X}(l) = 2(C-B)\overset{\tau}{y}$$

(19)

$$\ddot{X}(0) = 0 \;; \qquad \ddot{X}(l) = 0$$

(20)

where the *dot* denotes differentiation with respect to h. (The initial acceleration condition X(0) = 0 leads to p_2=0.)

The cartesian position, velocity and acceleration of the torch on the transition curve (as functions of the normalized time-step parameter h) are

[2] ITie transition equations are reproduced here because of the typographical errors in the cited reference.

$$X(h) = -(AC\overset{\tau}{Y} - AB)1V^{1} + 2(AC\wedge - AB)h^{3} + 2(AB)h + A \tag{21}$$

$$\dot{X}(h) = -4(AC\overset{\tau}{Y} - AB)h^{3} + 6(AC\overset{\tau}{Y} - AB)h^{2} + 2(AB) \tag{22}$$

and

$$\ddot{X}(h) = -12(AC\overset{\tau}{y} - AB)h^{2} + 12(AC\overset{\tau}{Y} - AB)h \tag{23}$$

where AB = (B - A) and AC = (C - B).

Filiation (21) defines the cartesian position of the torch (in terms of the normalized time-step parameter h) and is used to evaluate the coordinates of the transition point. The welding torch transits from the present segment to the next and maintains a continuous velocity and acceleration at the end points (A and D in F'igure 5) of the transition segments. Equation (21) is used to compute the position of tine torch during the transition. In the next section, the n, o and a vectors for the transition are formulated.

4. The Modified dT$_6$ Matrix

The dT$_6$ matrix specifics an incremental change in the orientation and position of the torch induced by incremental changes in die joint coordinates. Seam tracing requires incremental changes (in the base coordinates) in both the position and orientation of die torch. Since the changes in the base and the joint coordinates arc related through the nonlinear inverse Jacobian coordinate transformation, a small change in the position and orientation of the torch in the base coordinates may require a large change in the joint variables. This realization hampers application of the inverse Jacobian to compute the differential changes in the joint coordinates from the dT$_6$ matrix.

The goal of this section is to introduce the concept of a modified dT$_6$ matrix and an iterative algorithm which docs not restrict the nature of changes in the joint variables that led to the specified dT$_6$ matrix [Khosla 83]. If the changes are incremental (as assumed for the derivation of the inverse Jacobian), then the algorithm converges in the first iteration. Tn the case of large changes, the algorithm converges rapidly (in typically 2-3 iterations for the examples highlighted in Section 6) to the appropriate differential changes in the joint coordinates. The T$_6$ matrix at the next point is computed by adding the present T$_6$ matrix to the modified dT$_6$ matrix. This approach reduces computation time because computing the next $^{r}l'_{6}$ matrix does not require the forward solution.

Let R and S be two points on the mid-seam transition segment between the points A and D (in Figure 6).

Let tlie position and the orientation of the torch at points R and S be specified by T_{6R} and $T_{(S}$, respectively. LetT_{6S} be such that the change di$_6$ in T_{fiR} leads to T_{6S}. Thus,

$$Tes = T_{6R} + dT_6 \qquad (24)$$

It is also possible to reach T_{6S} from T_{6R} through a transformation C (in the base coordinates) which consists of a translation along the x, y and z axes followed by a rotation *0* along an axis k. Thus,

$$T_{6S} = CT_{6R} \qquad (25)$$

where

$$C \quad = Trans(x,y,z)Ro((k,0) \qquad (26)$$

Let n_R, o_R and a_R be the component vectors of the T_{6R} matrix specifying the orientation of the torch at the point R, and n_s, o_s and a_s be the corresponding vectors of the T_{6s} matrix. From (24), the corresponding differential vectors (In, do and da arc

$$\dot{d}h \;\text{--}i?_s \;\; -ti\vec{R} \qquad (27)$$

$$\vec{do} = \vec{Os} \;'' \vec{OR} \qquad (28)$$

$$\vec{da} \;\text{—}\vec{as} \; - \; a\vec{\wedge} \qquad \mathbf{(29)}$$

While traveling from point A to point D (in Figure 5), the dTV_u matrices should be computed to preserve the physical significance of the T_6 matrices at the transition points. Thus, T_{6R} should be computed from c!T_6 according to (24). Geometrically, the loci of the n, o and a vectors of a T_{fi} matrix should be a sphere of unit radius.

Figure 6 depicts the total desired change in each of the n, o and a vectors, while traversing from point A to point D (in Figure 5) in M steps. The components An, Ao and Aa, computed from (30)-(32), arc shown in Figure 6. The arc of the unit circle represents the loci of the n, o and a vectors during the transition. Let $(n_R)_u$, $(o_R)_u$ and $(a_R)_u$ be the unnormalizcd vectors whose tips lie on the point R^7 on the straight line joining points A and D. The subscript u indicates that the vectors arc unnormalizcd. The vectors n_R, o_R and a_R are obtained by normalizing the magnitude of the corresponding vectors to unit length.

The unnormalized vectors of the T_{6S} matrix are computed as

$$(n_s)_u=(n_r)_u+8n \tag{30}$$

$$(o_s)_u=(o_r)_u+8o \tag{31}$$

(32)

and then normalized to obtain the n_s, o_s and a_s vectors. 'l'hc right-hand sides of (27)-(29) are thereby specified completely, and the differential vectors of the dT_6 matrix can be computed to preserve the physical significance of the 'I'$_6$ matrix.

Having obtained the (In, do and da vectors of die dT_6 matrix in (15), it remains to compute the dp vector to specify completely the matrix. The vector dp is computed as

$$\vec{dp}=\vec{p}_S-\vec{p}_R$$

where the vectors p_R and p_s arc obtained from (21).

By construction, the d'lV$_6$ matrix satisfies (26). Since the magnitudes of the changes in the joint variables are *not* constrained in the derivation of the d'l'$_6$ matrix, the computed dT_6 matrix satisfies (27). Thus, the '1\ matrix at the next point S can be obtained by adding the T_6 matrix at the present point R to the computed dT_6 matrix (and consequently there is no need to compute the T_6 matrix at the point S from the updated values of the joint variables when the torch reaches the point S). The real-time computational requirements of this construction arc detailed in Section 5.

4.1. An Iterative Algorithm to Compute the Differential Changes

In applications, such as seam tracing (in which the sample points lie at incremental distances along the scam), tlie required changes in the joint variables may not be incremental. A practical example involves tracing a scam which has large slope variations. The dT_6 matrix is related to the changes in the joint variables through die inverse Jacobian which, in turn, is derived under the assumption of small changes in the joint variables. Many of the scams occurring in practice have slowly varying slopes and application of die inverse Jacobian to make the incremental motions is computationally advantageous. In practice, the scam may exhibit large slope changes at a few points, and the solution obtained (for the differential changes in the joint coordinates to reach the next point) from the inverse Jacobian may exhibit significant errors. The torch is thus placed at the incorrect point on the scam, and a large error (in the position and orientation of the torch) is introduced. To overcome this problem, an iterative algorithm is introduced. A block-diagram of the iterative algorithm is shown in Figure 7.

The algorithm begins at i = 0 with the initialization of the following variables: T_6* (T_6 matrix of the next point), T_{6i} (current T_6 matrix), and q_{i+A} (current values of the joint variables).

'Fhe algorithm implemented at the i-th iteration is ;

$$dT_{6} = T_{6}^{*} - T_{6i}$$

(33)

$$dQi+i = J"^{1}[dT_{6i},q,_{+}J$$

(34)

$$qi_{+}i = qi-kiq_{i+}i$$

(35)

$$T_{6}i=F[q_{i+1}]$$

(36)

$$qi=D[qi+i]$$

(37)

where $J"^{1}$ is the inverse Jacobian (in Table 5) for the computation of the differential changes in the joint variables from dT_{6i} and q_{j+J}. (in contrast to the symbolic or numerical inversion of the Jacobian matrix); F denotes the operation of computing the T_6 matrix (in Table 2); and D signifies the computation (delay) time for the forward solution.

Upon substituting (34) into (35),

$$Qi -hi = Qi + J\sim^{1}[dT_{6i},q_{i+1}]$$

(38)

and hence,

$$dq_{i+1} = (q_{i+1} - q_{i}) = J^{-1}[dT_{6i},q_{i+1}]$$

(39)

Equation (39), and consequendy the algorithm depicted in Figure 7, is the Ncwton-Raphson method [Atkinson 78] for solving the inverse Jacobian system of nonlinear equations (in Table 5).

The algorithm converges (in theory) when *all* of the components of the dT_{6i} matrix in the block-diagram (in Figure 7) arc zero. In practice, the algorithm is assumed to converge when each of die elements of dl'_{6i} is less than a prc-sct tolerance. The computed vector $</_{i}$ contains the desired set-points (in the joint variables) to reach the next position. When the desired changes in the joint variables arc small, the algorithm converges in one iteration and reduces to obtaining the inverse differential solutions from the inverse Jacobian (in Table 5).

For the scams tested with the simulator, the algorithm always converged in a maximum of three iterations (when the preset tolerance was set equal to zero). The computational requirements of the scam tracing algorithm are outlined in the next section.

5. Computational Requirements

The computations required to follow the scam from the present sample point to the next arc outlined in Table 6. The number of iterations required for the transition point computation and iterative algorithm (33)-(37) arc denoted by N_L and N_2, respectively. (For the scams traced by the simulator, typical values are found to be $N_{\{} = 2$ and $N_2 = 1$.) Execution times of the 8087 hardware instructions [Intel 83] are listed in Table 7. These floating point operation times (including the times required to load and store the operand) are used to estimate the time required to move the torch from one sample point to the next. Typical times (shown in Table 6) range from 24 to 29 milliseconds, which correspond to sampling rates of 35-40 Hz. For most welding applications, a sampling frequency of 10 Hz appears to be adequate.

These computational estimates are based upon the *matrix* kinematic modeling of manipulators used throughout this paper. Matrix representations of rotations arc highly redundant. *Quaternions [ftcclcv* 72, Hamilton 69] offer a convenient representation for rotations and can reduce both the storage requirements and computational load [Taylor 79]. The authors estimate that the quaternion implementation of the seam tracking algorithm would increase die achievable sampling rate to 60 Hz.

6. Simulation

To evaluate the algorithm, a software simulator has been developed (in the *C* programming language on a VAX 11/780) for the six degree-of-freedom Cyro robot in our laboratory. The simulation is initialized by retrieving scam data (as coordinates of sample points) from a data file. The first two sampled cross-sections of the seam are used to compute the desired T_6 matrix of the robot at the first point on the mid-seam and to compute the joint position and velocity set-points to reach die desired destination. Upon reaching the first point on the mid-seam, the algorithm computes the coordinates of the transition point on this segment (for the ratio T/T which is entered by the engineer at the start of the simulation) and the total time T required to traverse the next segment. The T_6 matrices at the present and next sample points are used to generate the joint position and velocity set points by the algorithm in (33)-(37). The trajectory from the beginning to end of the transition is computed from (21), and the joint position and velocity set-points arc computed to follow the interpolated curve. Upon reaching the end of the transition, the process is repeated (for each transition point), until the last sample point is reached. The simulation is then terminated and the specified curve is traced.

To achieve a quality weld, die lag or lead angle of the torch must be controlled adaptively. In the case of fillet and lap joints, the torch stand-off must also be controlled. Since an adaptive controller for these parameters remains to be developed, we have included (in our simu-latorXthe facility to specify these control parameters at the beginning of the simulation.

In the software simulator, the torch can be rotated about *two* axes. The first is about an axis *parallel* to the direction of travel and the second is about an axis *perpendicular* to the direction of travel (in the plane of the first axis). This capability allows control over the lead or lag angle of the torch. Facility to specify the stand-off for lap and fillet joints has also been incorporated. The simulator has tracked butt, lap and fillet joints and the experimental results arc highlighted in the next section.

7. Experimental Results

The seam tracking algorithm approximates the curve between sample points by a straight-line. To emphasize the effect of linear interpolation and the choice of sampling distance on the tracking accuracy, the simulator tracked a sinusoidal curve (with uniform spacings of 30 and 10 degrees). The simulation results arc depicted in Figures 8 and 9, respectively. As the sampling distance is *decreased*, the tracked curve approaches the actual curve. The maximum tracking error (which occurs for h = 0.5) is

$$\varepsilon = \frac{3}{16}\Delta C\frac{\tau}{T} - \frac{3}{16}\Delta B$$

and depends upon AB, AC and the ratio T/T. For a particular seam and sample points, AB and AC are constant and the tracking error (with respect to the interpolated curve) is a *linear* function of the ratio T/T. The simulation experiments illustrate that accurate tracking can be achieved by judiciously selecting the sample points and maintaining the ratio (T/T) of transition time to segment time as small as possible.

8. Conclusions

A general-purpose real-time seam tracing algorithm, for implementation on any six degrcc-of-freedom robot, is proposed. The algorithm (which requires knowledge of only one-point-ahead to track a seam) can be applied to a multitude of robotic seam tracking activities such as gluing, surface grinding and flame cutting. The algorithm incorporates the physical interpretation of the T_6 and dT_6 matrices to realize scam tracking. To reduce the computational requirements, the paper introduces the concept of a modified dT_6 matrix. The inverse Jacobian solution is generalized (according to Newton's method) to compute both large and small changes in the joint coordinates.

To test the efficacy of die proposed seam tracing algorithm, a simulator has been written and tested on a VAX 11/780. The simulation results arc highlighted in Section 7 of [Khosla 83]. The tracking accuracy is a function of the sampling distance because of the straight-line approximation between two successive sample points, and the tracking error increases with the increase in ratio of the transition time to the segment travel time.

Future activity will focus on die adaptive control of the weld parameters and dynamic robot control. Successful practical implementation will depend upon the availability of faster processors and the experimental performance evaluation of the algorithm.

References

[Agin 821 G. J. Agin and P.T. I lighnam.
A Movable Light Stripe Sensor for Obtaining Three Dimensional Coordinate Measurmcnts.
In *Proceedings ofSPIE: The Society ofOptical Engineers 360,* pages 326-333. San Diego, CA, August 21-27, 1982.

[Atkinson 78] K. R. Atkinson.
An Introduction to Numerical Analysis.
John Wiley and Sons, New York, 1978.

[Bccler72] M. Heeler, R. W. Gosper and R. Schrocppel.
"Hakmem".
Al Memo 239, Artificial Intelligence Laboratory, Massachusetts Institute of Technology, Cambridge, MA 02139, February, 1972.

[Bollingcf71] J. G. Bollingcr and II. L. Harrison.
Automated Welding Using Spacial Seam Tracings.
Welding Journal 50:787-792, November, 1971.

[Dcnavit 55] J. Dcnavit and R. S. Hartenberg.
A Kinematic Notation for Lower Pair Mechanisms Based on Matrices.
Journal of Applied Mechanics 11^{r}:215-221, June, 1955.

[Hamilton 69] W. R. Hamilton.
ElementsofQuaternions.
Chelsea Publishing Company, New York, 1969.

[Hill 80] J. W. Hill J. Krcmers and D. Nit/an.
Advanced Automation for Ship Building.
Final Report, Department of Navy Contract N00024-80-C-2026, SRI International, Menlo Park, CA 94025, November, 1980.

[Intel 83] *iAPX86/88, 186/188 User's Manual Hardware Reference*
Intel Corporation, 3065 Bowers Avenue, Santa Clara, CA 95051,1983.

[Khosla 83] P. K. Khosla.
Simulation of a Sensor Based Robotic Spatial Seam Tracing System.
Master's thesis, Department of Hlcctrical and Computer Engineering, Carncgic-Mcllon University, Pittsburgh, PA 15213, 1983.

[Masaki 79] I. Masaki.
Kawasaki Pais Memo No. 7904, Pais Center, Robot Group.
Technical Report, Kawasaki Heavy Industries Ltd., Japan, April, 1979.

[Masaki 81] I. Masaki, et al.
Arc Welding Robot with Vision.
In *PUeventh International Symposium on Industrial Robots,* pages 813-817. Tokyo, Japan, October 7-9, 1981.

[Paul 81] R. P. Paul.
Robot Manipulators: Mathematics, Programming and Control.
MIT Press, Cambridge, MA, 1981.

[Taylor 79] R.H.Taylor.
Planning and Execution of Straight Line Manipulator Trajectories.
IBM Journal ofResearch and Development 23(4):424-436, July, 1979.

[Tomi/uka 80] M. Tomizuka, D. Dornfcld and M. Porccll.
Application of Microcomputers to Automatic Weld Quality Control.
Journal ofDynamic Systems, Measurement, and Control 102(2):62-68, June, 1980.

[Whitney 72] D. F, Whitney.
The Mathematics of Coordinated Control of Prosthetic Arms and Manipulators.
Journal ofDynamic Systems, Measurement, and Control 94(4): 303-309, December, 1972.

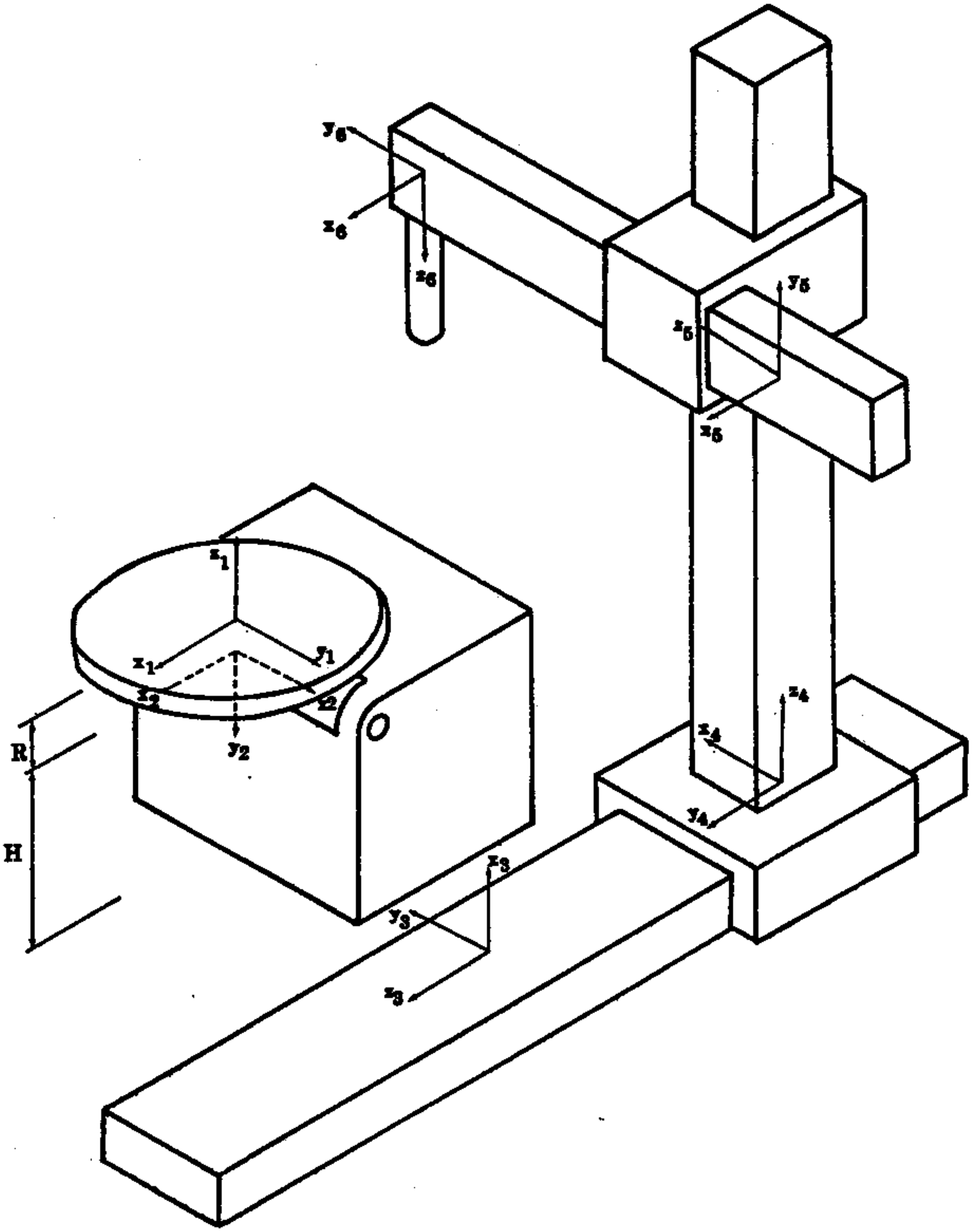

Figure 1: Link Coordinate Frames of the CYRO Robot

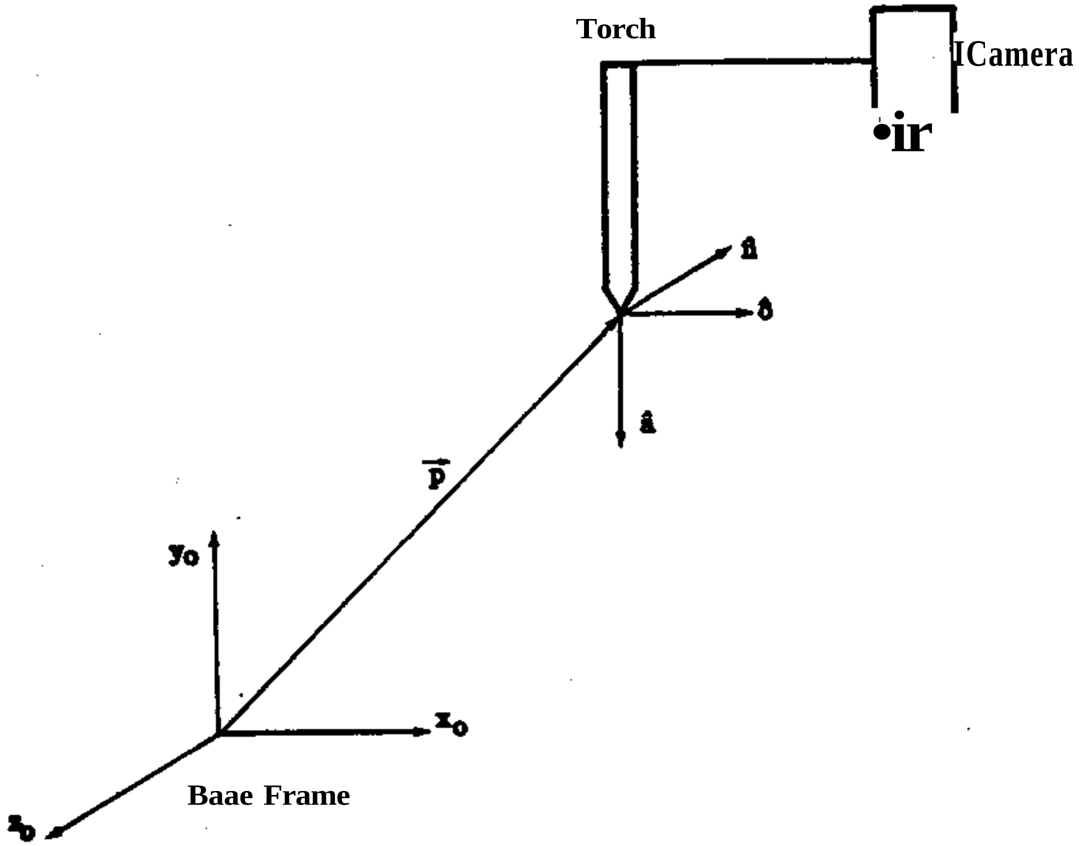

Figure 2: Physical Interpretation of the T_6 Matrix

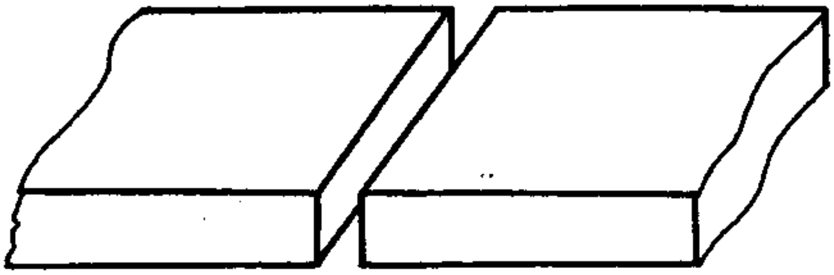

Figure 3: Butt Joint

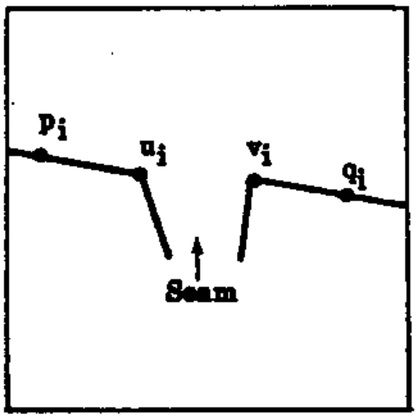

Figure 4: Camera Image of a Butt Joint

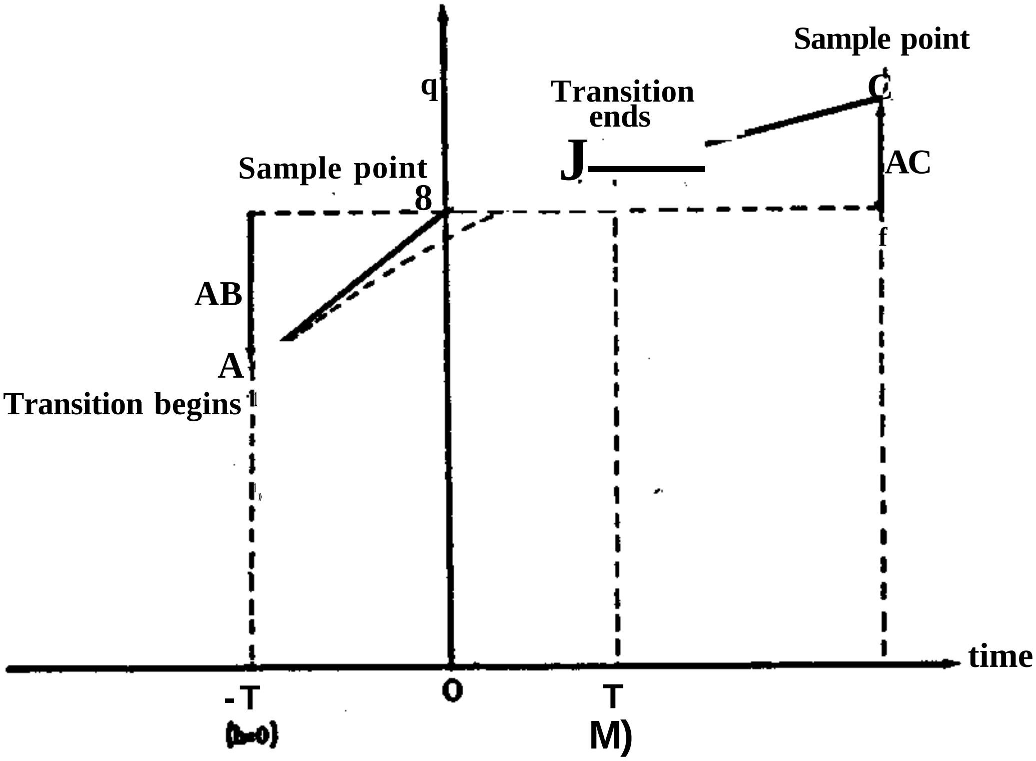

FigureS: A Transition Segment

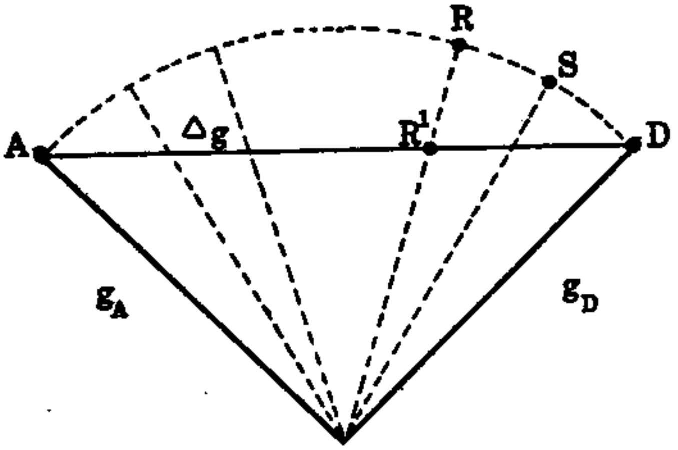

Note* The generic vector g symbolizes the normal (n), orientation (o) and approach (a) vectors.

Figure 6: Locii of n, **o** and a Vectors

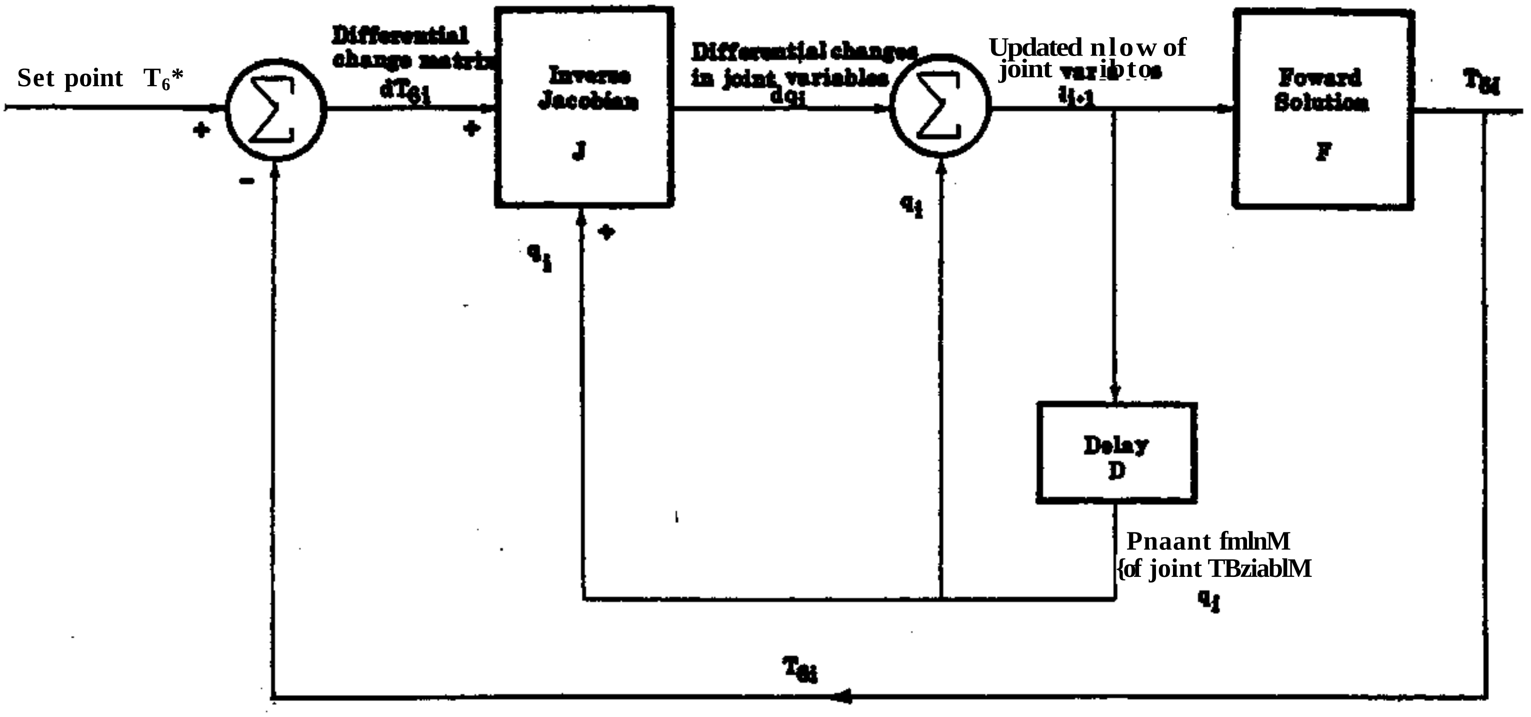
Set point T_6^*
+
-
Differential change matrix dT_{6i}
+
Inverse Jacobian
J
q_i
+
Differential changes in joint variables dq_i
q_i
Updated values of joint variables q_{i+1}
Foward Solution
F
T_{6i}
Delay
D
Present values of joint variables q_i
T_{6i}

Figure 7: Block Diagram of the Iterative Algorithm

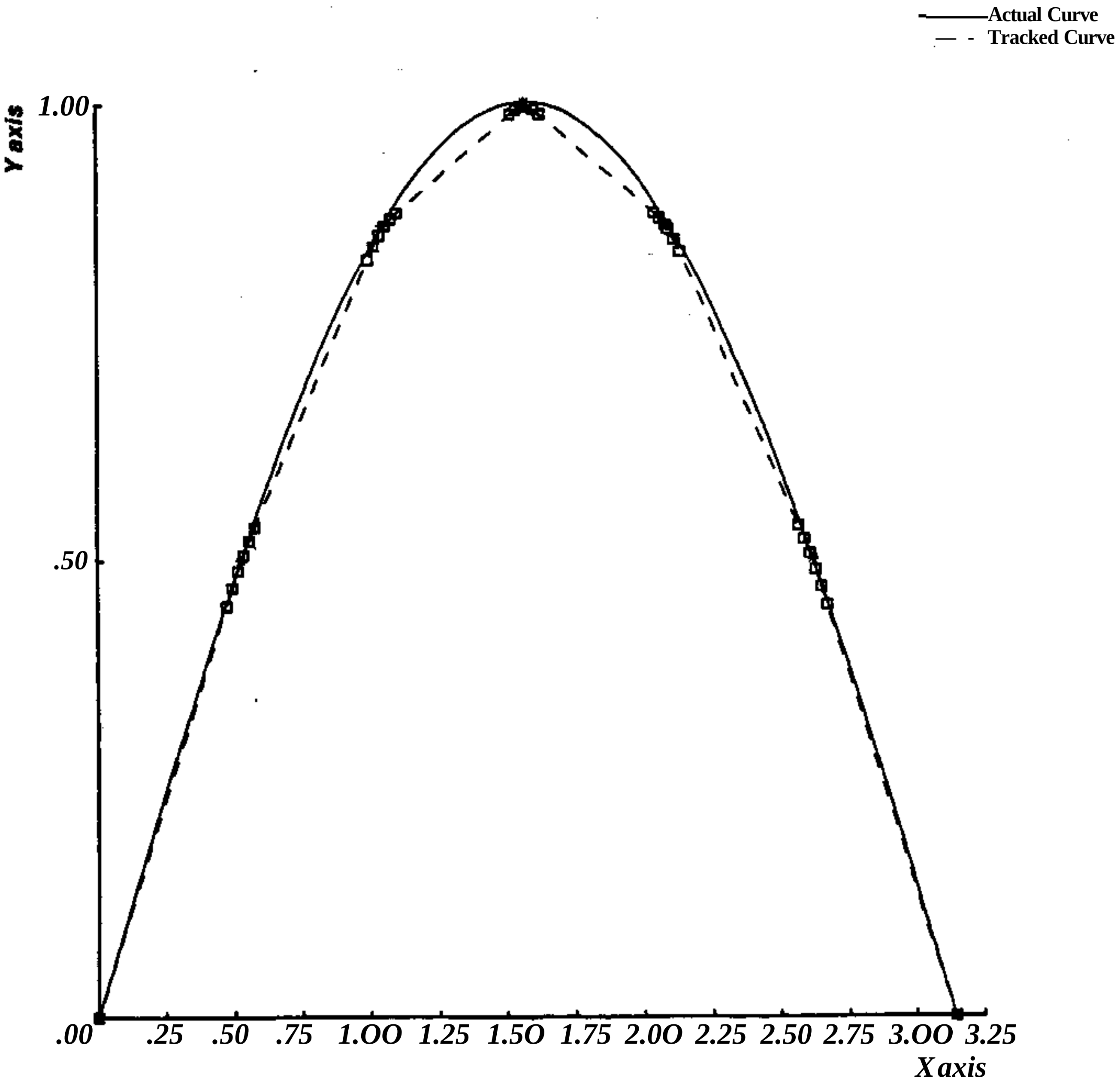

Figure 8: Sinusoidal Seam Tracking (30 degrees sampling interval)

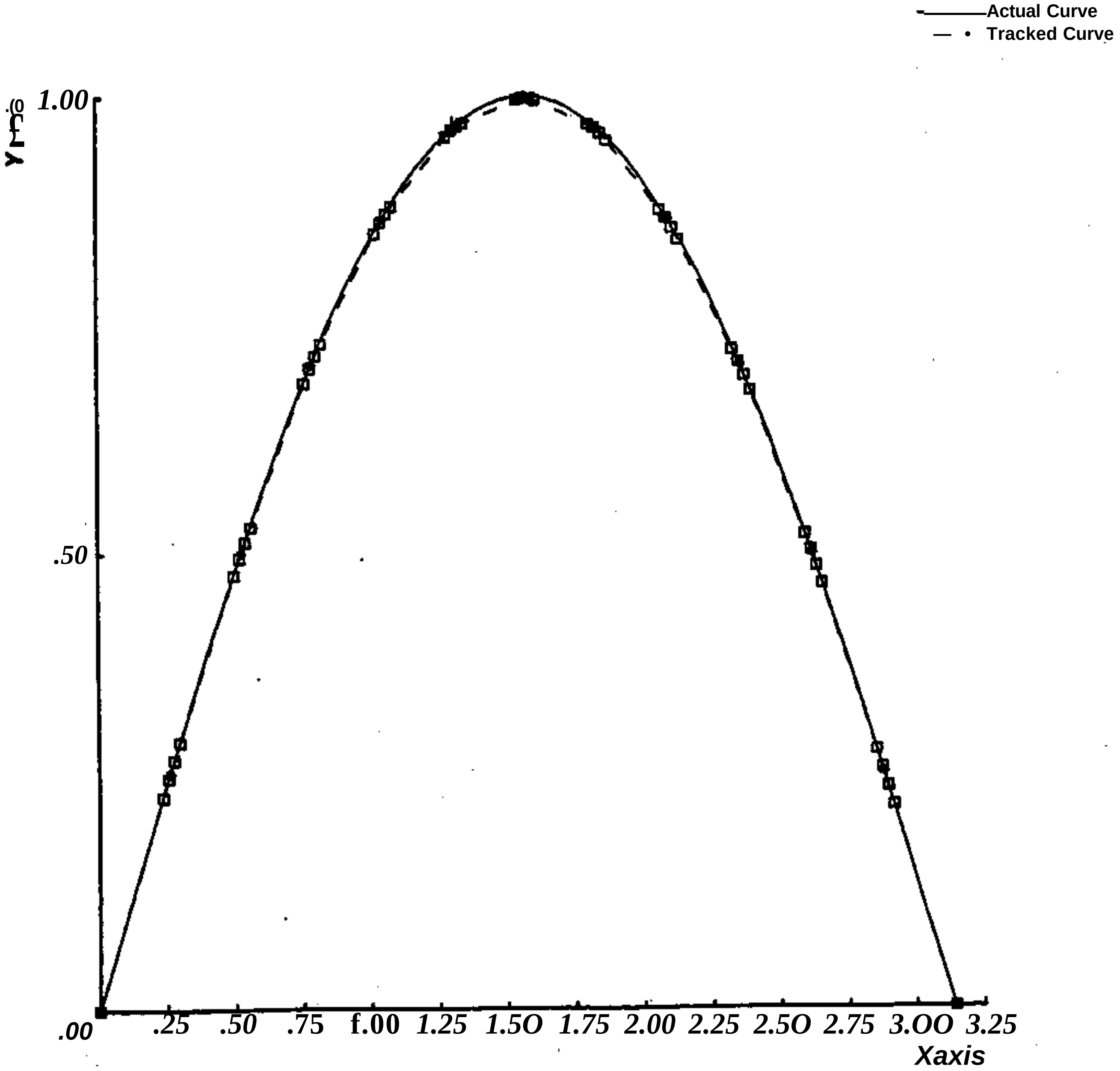

Figure* Sinusoidal Seam Tracking (10 degrees sampling interval)

Link	Variable	8	a	a	d
1	θ_1	θ_1	-90	0	-R.
2	θ_2	0_2-9O	-90	-H	L
3	*3	90	90	0	*3
4	*24*	90	90	0	*4
5	*ys*	0	0	0	*y%*
6	ft	ft	0	0	0

Definition of the Parameters

8 is the angle ofrotation about the raxis

a is the angle ofrotation about the x-axis

a is the length oftranslation along the x-axis

d is the length oftranslation along the z-axis

Table 1: Link Parameters of the CYRO Robot

$$
{}^{0}T_{6}=\begin{bmatrix} C_1C_2C_6+S_1S_6 & -CAS6+S_1C_6 & -C_1S_2 & C_1(z_4S_2 +X3Q -HSj) -Si(-y_5 +L) \\ S_1C_2C_6-C_1S_6 & -S_1C_2S_6-C_1C_6 & -S_1S_2 & 82(2482 +X3C2 -HSj)+Ci(-y_5 +L) \\ -S_2C_6 & S_2S_6 & -C_2 & (24C2-X_3S_2-HC2) -R \\ 0 & 0 & 0 & 1 \end{bmatrix}
$$

Table 2: Forward Solution of die CYRO Robot

Joint coordinate	Analytical Expression	Conditions
θ_1	$atan2\left[\frac{a_y}{a_x}\right]$	$7\text{-}_6(2,3)>$ 0
θ_1	$alanl\left[\frac{-q\ —Z\text{-}}{-a_x}\right]$	**$r_6(2,3)<$ 0**
0i	$atanl\left[\frac{-iC_{iax} \quad +S_{iay})]}{(-«,)}\ j\right.$	
x_3	$C_1C_2p_x + S_1C_2p_y - S_2p_z - S_2R$	
2A	$C\text{"'}Z?\text{-}ZT^{R+H}$	
y_5		
*	$atanl\left[\frac{o_z}{-n_z}\right]$	$8_2>$ 0
*	$atanl\left[\frac{o_z}{-n_z}\right]$ + 180°	^< . 0

NOMENCLATURE

C; is *the Cosine of the i-th joint angle*

Si is the Sine of the irth joint angle

atan2 is the double argument arc tangent junction

Table 3: Reverse Kinematic Solution of the CYRO Robot

$$\frac{\partial T_6}{\partial \theta_1}=\begin{bmatrix} \text{-<CiC}_2\text{C« +SiSt)(var]) +(SiC}_2\text{C6 - }C_1S_6)(var2) \\ -(C\dot{}_x\text{Ci\% +SAH>}^{arl}\text{> +("SiQS6 -QC6)(var2)} \\ \text{QS\^{}varl) -SjS}_2\text{(var2)} \\ -S_2C_6 \\ S_2S_6 \\ -C, \end{bmatrix}$$

$$\frac{3T«}{\partial \theta_2}=\begin{bmatrix} \text{-C}_2\text{Q(var3) +S}_2\text{Q(var4)} \\ \text{C|S|(var3) -SA<(var4)} \\ \text{SjCvari) -Cj(var4)} \\ -S_6 \\ \text{- Q} \\ 0 \end{bmatrix}$$

$$\frac{3]\wedge}{3*3}=\begin{bmatrix} C_6 \\ -S_6 \\ 0 \\ 0 \\ 0 \\ 0 \end{bmatrix} \qquad \frac{\partial T_6}{3*4}=\begin{bmatrix} 0 \\ 0 \\ -1 \\ 0 \\ 0 \\ 0 \end{bmatrix}$$

$$\frac{3T_6}{\partial y_5}=\begin{bmatrix} §6 \\ Q \\ 0 \\ 0 \\ 0 \\ 0 \end{bmatrix} \qquad \frac{HL}{30_6}=\begin{bmatrix} 0 \\ 0 \\ 0 \\ 0 \\ 0 \\ 1 \end{bmatrix}$$

NOMENCLATURE

varl =Si(z4Sj +x$_3$C$_2$ -HSj) +Q(-y$_5$ +L)

var2 sC$_1$(z$_4$S$_J$ +x$_3$Cj -HS2) +Si(-y$_3$ +L)

var3 =s - 24Q + X3S2 + HCj

var3 ^*uSj* +XjQ -HSj

TaMt4: Column Vectors of theJacobian matrix

DIFFERENTIAL JOINT COORDINATES

$$d\theta_1 = \frac{(-S_1da_x + C_1da_y)}{(C_1a_x + S_1a_y)}$$

$$d^{-}_{*} = \frac{NC_2d(NS_2) - NS_2d(NC_2)}{(NSJ^2 + (NC_2)^2}$$

$$dz_4 = C_2A_xd0_2 + S_2A_2 + C_2dp_z - S_2A_3d\theta_2$$

$$dy_5 = Cip_xd\$i + S\backslash dp_x + Sip_yd8i - C\backslash dp_y$$

$$d\theta_6 = \frac{C_6do_z + S_6dn_z}{S_6o_z - C_6n_z}$$

NOMENCLATURE

$$NC_2 = -a_t$$

$$d(NC_{2)} = -da_t$$

NS2 = """"""Cltfx — •S'l^y

$$d(NS_{2)} = S\backslash Q_xd0\backslash — C\backslash d(i_x — C\backslash ciyCi\$x - S\backslash da_y$$

$$A\backslash = C\backslash p_x + S\backslash Py$$

$$A_2 = \sim\sim Slp_Xd\$l + C\backslash dp_x + C\backslash Pydth+Sidpy$$

Table 5: Inverse Jacobian of the CYRO Robot

STEP	*	-h	÷	√	SIN/ /cos	TIMHin millisec
Find the mid-scam						
Butt Joint (1)		'3	3			0.384
Lap/Fillet Joint (2)	3	6				0.462
Compute segment travel time T						
Butt Joint	23	39	I	5		3.611
Lap/Fillet Joint	32	61	1	6		5.256
Find transition point						
Butt Joint	23*N i	39*N,	**Nt**	5*N ,		7.222
Lap/Fillet Joint	32*N_t	6l*Ni	**Ni**	6*N_V		10.512
Computation of						
a Vector	9	14	5	1		1.611
o Vector (6)-(7)	15	11	3	1		1.675
n Vector (8)	3	6				0.462
Compute dT $_6$ Matrix		12				0.576
Normalization	9	4	3	3		1.125
Iterative algorithm (33) - (37)	66*N_2	54*N_2			6*N_2	7.206
'Total						
Butt Joint	62 + 23*Nt + 66*N_2	86 + 39*N, + 54*N_2	15 + N,	**10 + Nj**	6*N_2	23.872
Lap/Fillet Joint	73+23*Ni + 66*$N_?$	108 + 39*Ni + 54*N_2	15 + N,	10 + N,	6*N_2	28.885

Table 6: Computational Requirements of the Scam Tracing Algorithm

An Algorithm for Seam Tracking Applications

P. K. Khosla, C. P. Neuman, and F. B. Prinz

CMU-RI-TR-84-6

The Robotics Institute
Carnegie-Mellon University
Pittsburgh, Pennsylvania 15213

May 1984

This work has been supported by the Inlaks Foundation, U. K., and the Department of Electrical and Computer Engineering and Welding Consortium, Robotics Institute, Carnegie-Mellon University.

Table of Contents

List of Figures

List of Tables

Abstract

Seam tracking is currently accomplished by special features of the robot and *a priori* knowledge of seam geometry. In this paper we demonstrate the feasibility of tracking a seam in real-time. A general-purpose seam tracking algorithm is developed for implementation on a robot with six degrees-of-freedom. The algorithm is motivated by a physical interpretation of the T_6 and dT_6 matrices, and the assumption that 3-D seam data are available. In the past, the dTV matrix and inverse Jacobian solutions have been used to compute the differential changes in the joint angles. By using the inverse Jacobian, an iterative algorithm is introduced to compute both large and small changes in the joint variables. The versatile seam tracking algorithm can be applied to a multitude of robotic seam tracking activities such as gluing, surface grinding and flame cutting.

1. Introduction

Manufacturing operations such as robotic welding, gluing, sealing and surface grinding require trajectory control of the tool mounted on the end-effector of the robot. While the kinematic control algorithm developed in this paper is applicable to a multitude of manufacturing operations, robotic arc welding nomenclature is used. The tool is called the welding torch, and the tool trajectory is defined by the weld scam. The fundamental problem is to position a welding gun with the proper translational and rotational positions with respect to a curved weld scam in three dimensional (3-D) space. A scam in space can be traced by a five degrcc-of-freedom robot. Since real-time seam tracing requires that *both* the sensor *and* torch trace the seam, a six degrcc-of-freedom robot is required. Automation of the welding process thus demands a robot with *six* degrces-of-freedom and acceptable performance in terms of speed and accuracy. The control task also demands a *real-time* algorithm to guide the robot in a fixed geometrical relationship to die contour.

Automation of the welding process can be divided into two distinct components :

- Scam data acquisition and interpretation by a sensor system ; and
- Guidance* and control of the robot to traverse the seam, while maintaining the proper orientation and position.

Since the scam data constitute the 3-D coordinates of the seam, a visual sensory device (such as a light stripe imaging device) can be used to obtain the seam data. Methods for obtaining 3-D data from 2-D images have been developed [Agin 82]. Having obtained and interpreted the scam data, the control system must guide die robot to traverse the scam and place the requisite amount of weld material along the path. The torch position and attitude must be controlled precisely to ensure acceptable weld quality.

Scam tracking is currently accomplished by exploiting a special feature of the robot or limiting the application to a particular type of a seam. Bollingcr and Harrison [Bollinger 71] describe the principles and techniques of a spatial scam tracking system. In this application, the seam is constrained to lie on a cylindrical surface. Tomi/.uka, *et ah* [Tomizuka 80] propose a preview control strategy for two-axis welding torch positioning and velocity control. The scheme is only applicable for two-axis control and hence constrains the scam to lie in a plane. Furthermore, the scheme cannot be implemented on a general purpose six degrcc-of-frccdom robot.

One of the first successful demonstrations of computer vision to arc welding is the NASA *weld skate [HWl* 80]. This system has been implemented on a special-purpose robot and requires special edge preparation to operate properly. The system is incapable of making any determination regarding the joint fit-up. The principle of structured illumination has been employed by Kawasaki Heavy Industries of Japan [Masaki 79] to develop a visual seam tracking system. The approach used for image analysis is *training-by-showiug.* A set of typical images is acquired in a teaching operation prior to welding and stored in the memory of the processor. As real-time images are acquired, a search is conducted (through the set of trained images) until a match is found. During the matching process, the positional displacement between the two images is computed and used to correct the position of the torch. The system has been designed specifically for the ship building industry and hence operates only on fillet joints. The system does not utilize part fit-up information for seam tracking.

An example of wclding-by-tcaching is the system described by Masaki, *et al* [Masaki 81] which has a visual scam tracking capability. The robot is taught the reference path for the end-effector and the reference image for the image processor. In the teach mode, two passes arc required for each work piece, one for sensing and one for welding. The path for the welding operation is generated from the sensing pass information.

Current robot welding systems are thus suitable for large batches of parts which are cut and fit to tight tolerances. The robot must trace and weld a scam, within acceptable tolerance limits, on such closely fit parts. Another limiting factor for a semi-automated welding system is the robot programming and set-up time in the shop when the part is changed. These constraints may be eased through the introduction of a CAD/CAM data base in which tlie welding trajectories and speed, weave pattern, wire feed rate, voltage and current are stored for each welding part and then retrieved as required. Unpredictable fit-up and loose part tolerances create the need for a real-time guidance and control algorithm.

The objective of this paper is to introduce a versatile scam tracing algorithm that demonstrates the feasibility of tracking a scam in real-time. The general purpose seam tracing algorithm can be implcmcntablcd on any robot with six degrccs-of-freedom. The algorithm is motivated by the physical interpretation of tlie forward solution, or T_6 matrix [Paul 81] and tlie inverse Jacobian. To facilitate implementation of the inverse Jacobian solutions, an iterative algorithm is developed to compute the differential changes in the joint variables from tlie dT_6 matrix. To reduce significantly the on-line computational requirements, the concept of a modified dT_6 matrix is also introduced. To evaluate the performance of the scam tracing algorithm, a functional simulation package (for the Cyro[1] robot in our laboratory) has been implemented. The outputs of tlie simulation arc the joint position and velocity set-points for tlie robot control system.

The paper is organized as follows. The kinematics of the Cyro robot (including the forward and reverse solutions , and the Jacobian and inverse Jacobian) are developed in Section 2. The foundations for the scam tracking algorithm are laid in Section 3. Focus is on the specification of the T_6 matrices at tlie sample points

[1] **Cyro is a trademark of the Advanced Robotics Corporation.**

along the seam and planning the motion of the torch. To reduce the computational requirements of the algorithm for real-time applications, the concept of the modified dT_6 matrix is introduced in Section 4, and an iterative algorithm to compute both large and small changes in the joint coordinates is then developed. The computational requirements arc enumerated to indicate the potential for die real-time implementation of the algorithm. The salient features of the simulator, which has been implemented to evaluate the performance of the scam tracing algorithm, arc presented in Section 5. Simulation experiments for representative test cases are then highlighted in Section 6. Finally, in Section 7, conclusions arc drawn from the simulation experiments, and the paper is summarized.

2. Kinematics of the Cyro Robot

The forward solution (or T_6 matrix) of die robot, from the base frame to the torch (or end-effector) frame, is developed using homogeneous transformations [Paul 81]. The homogeneous transformations, relating two successive coordinate frames, are only a function of the six joint coordinates. Thus, knowledge of all of the six joint coordinates leads to the transformation (or forward solution) from the base frame to the torch frame.

To develop the homogeneous transformation or A matrices, a coordinate frame is embedded in each of the six links of the robot, using the Dcnavit-Hartcnbcrg convention [Dcnavit 55]. The coordinate frames are shown in Figure 1. Joints 1,* 2 and 6 are rcvolute, and joints 3, 4 and 5 are prismatic. The coordinates of the rcvolute joints arc $\#_1$, $\$_2$ and $0'_6$ and the coordinates of the prismatic joints are $x\sim_3$, z_4 and yy_5. The subscripts on the coordinates indicate the joint number; the base is link zero. The base coordinate frame is fixed at the center of the table of the robot and coincides with the first coordinate frame. When *all* of the six joint coordinates arc zero, the axes for joint 1 (table) and joint 6 (torch) arc parallel and the robot becomes singular. In the algorithm, the manipulator is assumed to be at the zero position. Without loss of generality, the constant offsets of die robot are assumed to be zero. A counter-clockwise rotation of the revolute joints is considered to be positive,, and translation of die prismatic joints along the positive z-axis is considered to be positive.

The link parameters of the Cyro robot arc listed in Table 1, and the forward solution is displayed in Table 2. Having obtained the forward solution, the values of the joint coordinates that led to the $1"_6$ matrix can be computed. This reverse solution [Paul 81] is required (by the simulator) to relate the T_6 matrix to the present values of the joint coordinates. The reverse solution is listed in Table 3.

The differential changes in the cartesian coordinates of the torch are related to the differential changes in the joint coordinates through the manipulator Jacobian [Whitney 72, Paul 81]. Each column of the Jacobian matrix J is a differential translation and rotation vector. The column vectors of

$$J = \begin{bmatrix} \frac{\partial T_6}{\partial \theta_1} & \frac{9T_6}{9\#2} & \frac{9T_6}{9\wedge 3} & \frac{9T_6}{9z_4} & \frac{9T_6}{9y_5} & \frac{9T_6}{9\#_6} \end{bmatrix}$$

arc listed in Table 4.

In scam tracing, sensory data can be utilized to determine the incremental change in the position of die seam from differential changes in the elements of the T_{fi} matrix. The differential change matrix dT_6 is thus available tri plan the incremental motions of the torch. It thus becomes imperative to find the inverse Jacobian (or incremental changes in the joint coordinates) which produce the specified incremental change in the $\underset{0}{T,}$ matrix.

Numerical inversion of die Jacobian [Whitney 72] is computationally intensive and hence is not suitable for real-time control applications. Incremental changes in the joint coordinates can be obtained from a Taylor scries expansion of the reverse solution. Such an approach leads to analytical formulae for the differential joint coordinates which are functions of the elements of the T_6 and dT_6 matrices [Paul 81]. Analytical formulae for the differential joint coordinates, which arc obtained by differentiating the reverse solution (in Table 3), are listed in Table 5.

3. Kinematic Seam Tracking Control

The control task is to fill a volume with weld material while maintaining the proper position and orientation of the torch with respect to the seam. While traversing the seam, the tip of the torch traces a curve in 3-D space. If the discrete points on the curve to be traced and the surface containing the curve arc identified, the T_6 matrices can be generated for each point on the discrctized curve.

Specification of the T_6 matrices at the sample points of the discretized curve accomplishes die seam tracing task. The $\underset{0}{T_A}$ matrix is

$$T_6 = \begin{bmatrix} n & o & a & p \\ 0 & 0 & 0 & 1 \end{bmatrix} = \begin{bmatrix} n_x & o_x & a_x & p_x \\ n_y & {}^{o}y & a_y & P_y \\ n_z & o_7. & a_7. & P/. \\ 0 & 0 & 0 & 1 \end{bmatrix}$$

and represents the position and orientation of the torch shown in Figure 2. The origin of the describing coordinate frame is located at the tip of the torch and is described by the vector p with respect to the base frame. The three unit vectors n, o and a, which describe the orientation relative to the base frame, are directed as follows [Paul 81]. The z-axis of the describing frame lies along the direction that the torch approaches die surface (containing the curve to be traced) and is called the approach vector a. The y-axis of the describing frame lies along the direction of the boom holding the camera and is called die orientation vector o. The normal vector n is then chosen to form a right-handed set of vectors and is computed as

$$\tilde{t}t = 3 \times 3$$

The vectors n, o and a describing the orientation of the torch and the vector p describing the position can be specified independently. The control task can thus be split into two independent components :

- Tracing a curve in 3-D space; and
- Maintaining proper orientation of the torch with respect to die surface which contains the curve to be traced.

The volume to be filled with the weld material is contained within two surfaces (of metal) which arc to be joined together. The surfaces may be non-overlapping, as in the case of a butt joint (in Figure 3), or overlapping as in the case of a lap joint or a fillet joint.

Let *m* be a curve (in 3-D space) which lies on the surface *S* and is to be tiaccd by the tip of the torch. The surface *S* may have a varying slope. Henceforth, the curve *m* will be termed the *mid-seam.* The mid-scam is discrcti/cd length-wise. Let nr$_i$ be the vector (with respect to the base frame) pointing to the i-th sample point m$_i$ on the mid-scam. The discretization is specified to allow a picccwisc linear approximation of the curve *m* between two adjacent sample points. If the surface (in the vicinity of the two sample points tn.$_i$ and m.$_{i+i}$) is also discrctized, then a pieccwisc planar approximation of *S* is obtained. Let *P*$_i$ denote the plane (containing the points m$_i$ and m$_{i+}$ j). The direction cosines of the plane specify the orientation of the torch which is held constant for the duration of travel from m.$_i$ to m$_{i+i}$.

The position of the torch is specified by the coordinates of the sample points. The foregoing description of the position and the orientation of the torch completes the formulation of the T_6 matrix at die sample points. The ensuing section specifics the T_6 matrix for butt, lap and fillet joints.

3.1. Specification of the T_6 Matrix

Having interpreted physically the elements of the T_6 matrix, die next step is to generate numerical values of the elements of the T_6 matrix in terms of the coordinates of the sample points obtained from the sensor system. Since a light stripe projector and a solid state camera are assumed to be used as the sensory device, the 3-D coordinates of the points on the surfaces to be joined arc mapped into pixels in the camera image. Figure 4 shows a typical camera image (at the i-th sampling instant) obtained from a butt joint. The break points in the camera images of the surface indicate the discontinuity in *the* actual surfaces to be welded. To specify the curve to be traced, it is essential to extract 3-D coordinates of the break points in the images. The information regarding the orientation of the surfaces, in the vicinity of the break points, can be obtained by extracting the coordinates of one additional point on each surface. The break points are called $u_{.1}$ and v_i for the butt joint shown in Figure 3. The additional points on each of the two surfaces arc called p_t and *q*.^ respectively. The subscript i denotes the sampling instant. The coordinates of the sample points are specified with respect to the base frame of the robot, and $p_{.i}$, $u_{.i}$, $v_{.i}$ and $q_{.i}$ arc die vectors from the origin of the base frame to the points p_p $u_{.,i}$ $v_{.i}$ and $q_{\{}$ respectively. The edges formed by die sample points { $p_{.i}$ }, { $q_{.\{}$ }, { $u_{.i}$ } and { $v_{.i}$ } arc denoted by /?, r/, M, and v, respectively.

To specify the p vector of the T_6 matrix requires knowledge of the sample points along the mid-scam. For a butt joint, the requirement that the torch be placed exactly in the middle across the *u* and v edges forces the x, y and z coordinates of the mid-seam to be computed as:

$$m_{xi} = \frac{u_{xi} + {}^{v}xi}{2}$$
$$m_{yi} = \frac{u_{yi} + v_{yi}}{2}$$
$$m_{rr} \cdot \approx \frac{u_{zi} + v_{zi}}{2}$$

0)

For both lap and fillet joints, torch stand-off is an important consideration for obtaining a quality weld. Let the desired torch stand-off be characterized by the parameter s, where s ranges from 0 to 1. The coordinates of the mid-seam are then computed as

$$m_{xi} = u_{xi} + s(v_{xi} - u_{xi})$$
$$m_{yi} = u_{yi} + s(v_{yi} - u_{yi})$$
$$m_{zi} = u_{zi} + s(v_{zi} - u_{zi})$$

(2)

The $p^x_;$ p^y and p_z components of the T_6 matrix are

$$Px = {}^{m}xi \qquad \wedge^3>$$

$$p_z = m_{zi} \qquad (\cup)$$

and specify completely the last column of the T_6 matrix.

Practical seams have edges with slowly-varying slopes. Since the sample points are assumed to lie close to each other (typically separated by 1 mm), the edges between two sample points can be approximated by a straight line. This approximation leads to a planc which Passes thl0ll Sh at least ^ircc of the four sample points (Pi, p.+,, q., qi+ {). The direction cosir. *CS of ^ planc arc also thc direction cosi » cs of a vector normal to the plane. Since'the torch is required to be \DC1 Pcndicular "> the *fictitious* scam surface, thc direction cosines of thc approach vector a are specified as th'° *negalive* of thc dircction cosincs * ^ normal to thc plane.

Thc values of thc components of thc orientation vector o ^ computcd under ^ following constraint. When thc torch and the camera arc on thc seam, both should trac k tho SCam, This condition guarantees that sample points will not be lost if the slope of thc mid-edge (at thc poi'nt of thC torch) dlffcrs from thc slope at thc point-of-vicw of thc camera. Let M be a constant shift in thc numbc."of sam P|c P()i«ts between thc torch and thc camera. Figure 2 shows that the o vector is perpendicular to tl.>e a vcctor and points along thc direction of the arm holding the camera. If thc camera is traveling in the direction o* L1C line joining in_{i+N-1} and m_{i+N}, then tlic robot system will never lose track of the scam, unless thc slope experiences large changes or discontinuities along thc scam.

The equation of a plane passing through three of thc four points (p_{i+1V} Pj_{+1}\-v Q_{+} *w* ^i + N-l^ can now ^e specified, and **tlic** angle between thc planes at thc camera and the torch points can be determined. If *$(X_v$* /x_r *$v_{\{})$* and (X_2, ju_2, *vj* arc thc dircction cosincs of thc two planes, then thc cosine of angle *0* between thc planes is

cos(0) =XiA2 +/MM2 +^1^2

(6)

Thc vector a joining the points ni_{j+N-1} and m_{i+N} along thc mid-edge is computed as

$$\vec{a} = \vec{m}_{i+N} - \vec{m}_{i+N-1}$$

(7)

The projection of the vector a onto thc torch plane is chosen to be the o vector and is normalized to be of unit length. Having obtained the normalized o and a vectors, tlic n vector is computed as

a = 3 x 3

(8)

to specify completely the T_6 matrix at the sample points.

While traversing from the i-th to the (i-f-l)-th point, die orientation of thc torch and consequently tlic n, o and a vectors remain constant. The p vector in the T_6 matrix changes linearly because of thc straight line approximation between the two points. To maintain a continuous speed and acceleration at **tlic** end points of the segment, the motion of the torch is planned.

3.2. Planning the Motion of the Torch

ThP mnrinn of the tio of thc torch, in traversing a scgr; # I ne motion 01 me up ui {Qn^ |S composcc| of two parts:

- Motion along the segment, and
- Transition between segments.

To make a smooth transition bctwo ^ scgmcnts< jt js desirable to maintain a continuous velocity and acceleration at the transition points. To spccify thc transition equations, a fourth-order curve is fit between the point where a transition star'tS-"an(j ^Q po jnt jnc|jcaljng thc end of thc transition [Paul 81]. The equations for thc transition trajcctorics> ancj velocities arc outlined in Section 3.3.

Let M be thc totorf number of transition steps in which thc desired change in T_6 is to occur. The differential changes in the $v_t(o$ and a vectors at each transition point are

$$\Delta\vec{n} = \frac{\vec{n}_{(i+1)} - \vec{n}_i}{M} \tag{9}$$

$$A! = \frac{\vec{a}_{(i+1)} - \vec{a}_i}{M} \tag{10}$$

$$A3 = \frac{\vec{o}_{(i+1)} - \vec{o}_i}{M} \tag{11}$$

where the subscripts i and (i + 1) denote the i-th and (i + l)-th segments, respectively. 'Hie An, Ao and Aa vectors arc then added to die current n, o and a vectors, respectively, and normalized to unit length, to produce thc n, o and a vectors at the next segment. Let n_p, o_p, a_p and n_n, o_n, a_n be thc vectors of the T_6 matrix at thc present and next segments, respectively; and let thc subscript N indicate that these vectors have been normalized to unit length. The n_u, o_n and a_n vectors arc thus computed as follows :

$$fin = (rtp + \vec{An})_N \tag{12}$$

$$\vec{o}_n = (\vec{o}_p + \vec{\Delta o})_N \tag{13}$$

$$\vec{a}_n = (\vec{a}_p + \vec{A}a)_N \tag{14}$$

Having computed the three component vectors (n, o and a) of T_6 at the next segment, the first three columns of the differential change matrix dT_6 are determined, and the fourth column (or dp vector) can be computed from the transition trajectory to specify the differential translation. The differential change matrix dT_6 is then

$$dT_6 = \begin{bmatrix} dn_x & do_x & da_x & dp_x \\ dn_y & do_y & da_y & dp_y \\ dn_z & do_z & da_7 & dp, \\ 0 & 0 & 0 & 0 \end{bmatrix} \tag{15}$$

where the differential vector components (dn, do, da and dp) of the dT_6 matrix represent the corresponding change in the vector components (n, o, a and p) of the T_6 matrix.

Having generated the present T_6 matrix and d'l $_6$ matrix to reach the next point, the inverse Jacobian (in Table 5) is used to compute *iterative!)'* the differential changes in the joint coordinates. 'The inverse Jacobian solutions arc derived under the assumption that the changes in the joint variables leading to the specified dT_6 matrix are *small.* To overcome the practical fact that this assumption is *not* always satisfied in scam tracing applications, an iterative technique is developed to compute the changes in the joint variables. The velocity set-points during the transition are obtained by dividing the incremental values of the joint variables by the time required to make the incremental change. The transition ends when the torch reaches the point D on the segment B-C in Figure 5. At this point, the torch has the required orientation and velocity to track the (i + l)-di segment I>C without error. This motion is called *motion-along-the-segment.*

During the motion of the torch, along the segment, the n, o and a vectors of the-robot remain constant. The updated dT_6 matrix is specified as:

$$<n'6= \begin{bmatrix} 0 & 0 & 0 & dp_x \\ 0 & 0 & 0 & dp_y \\ 0 & 0 & 0 & dp_z \\ 0 & 0 & 0 & 0 \end{bmatrix} \tag{16}$$

where d p.. dp_v and dp., arc the differential changes in the x, y and z coordinates of the (i + l)-th transition point. When the torch reaches the next transition point, the process of planning the motion of the torch, along the segment and during the transition, is repeated to plan the motion for the next segment.

3.3. The Transition Curves

A transition segment is illustrated in Figure 5. The transition starts at point A in the i-th segment and ends at point D in the (i-f l)-th segment. Maintaining a continuous velocity and acceleration at the points A and D appears to require that six boundary conditions be satisfied. A fifth-order polynomial (with six parameters) would then be needed to approximate the cartesian transition curve. *Symmetry* of the transition guarantees that a *quartic* polynomial can approximate the cartesian transition curve [Paul 81|[2]. To facilitate the development, let T be the transition time and T be the time required to traverse the segment ft-C. The time of travci (T) across a segment is computed by dividing the volume of the weld material (to be deposited along the segment) by the weld-wire volumetric feed-rate, which is assumed to be constant. 'The ratio (r/T) is specified by the engineer (in Section 6). Let the *normalized* time-step parameter h be defined according to

$$h = \frac{t + \tau}{2T} \qquad (17)$$

where t denotes the running time-variable (-T < t < T).

Let the fourth-order polynomial approximating the cartesian transition segment be

$$X(h) = \beta_4 h^4 + \beta_3 h^3 + \beta_2 h^2 + \beta_1 h + \beta_0$$

where the five parameters (*fi*$_i$ for i = 0 to 4) must be selected for X(h) to satisfy the boundary conditions [Paul 81]:

$$X(0) = A \; ; \qquad X(l) = (C-B)\hat{}r + B \qquad (18)$$

$$\dot{X}(0) = 2(B-A) \; ; \qquad \dot{X}(l) = 2(C-B)\overset{\tau}{y} \qquad (19)$$

$$\ddot{X}(0) = 0 \; ; \qquad \ddot{X}(l) = 0 \qquad (20)$$

where the *dot* denotes differentiation with respect to h. (The initial acceleration condition X(0) = 0 leads to $p_2 = 0$.)

The cartesian position, velocity and acceleration of the torch on the transition curve (as functions of the normalized time-step parameter h) are

[2] **ITie transition equations are reproduced here because of the typographical errors in the cited reference.**

$$X(h) = -(AC\overset{\tau}{Y} - AB)1V^{1} + 2(AC\wedge - AB)h^{3} + 2(AB)h + A$$

(21)

$$\dot{X}(h) = -4(AC\overset{\tau}{Y} - AB)h^{3} + 6(AC\overset{\tau}{Y} - AB)h^{2} + 2(AB)$$

(22)

and

$$\ddot{X}(h) = -12(AC\overset{\tau}{y} - AB)h^{2} + 12(AC\overset{\tau}{Y} - AB)h$$

(23)

where AB = (B - A) and AC = (C - B).

Filiation (21) defines the cartesian position of the torch (in terms of the normalized time-step parameter h) and is used to evaluate the coordinates of the transition point. The welding torch transits from the present segment to the next and maintains a continuous velocity and acceleration at the end points (A and D in Figure 5) of the transition segments. Equation (21) is used to compute the position of tine torch during the transition. In the next section, the n, o and a vectors for the transition are formulated.

4. The Modified dT_6 Matrix

The dT_6 matrix specifics an incremental change in the orientation and position of the torch induced by incremental changes in die joint coordinates. Seam tracing requires incremental changes (in the base coordinates) in both the position and orientation of die torch. Since the changes in the base and the joint coordinates arc related through the nonlinear inverse Jacobian coordinate transformation, a small change in the position and orientation of the torch in the base coordinates may require a large change in the joint variables. This realization hampers application of the inverse Jacobian to compute the differential changes in the joint coordinates from the dT_6 matrix.

The goal of this section is to introduce the concept of a modified dT_6 matrix and an iterative algorithm which docs not restrict the nature of changes in the joint variables that led to the specified dT_6 matrix [Khosla 83]. If the changes are incremental (as assumed for the derivation of the inverse Jacobian), then the algorithm converges in the first iteration. Tn the case of large changes, the algorithm converges rapidly (in typically 2-3 iterations for the examples highlighted in Section 6) to the appropriate differential changes in the joint coordinates. The T_6 matrix at the next point is computed by adding the present T_6 matrix to the modified dT_6 matrix. This approach reduces computation time because computing the next $^{r}l'_{6}$ matrix does not require the forward solution.

Let R and S be two points on the mid-seam transition segment between the points A and D (in Figure 6).

Let tlie position and the orientation of the torch at points R and S be specified by T_{6R} and $T_{(S}$, respectively. LetT_{6S} be such that the change di$_6$ in T_{fiR} leads to T_{6S}. Thus,

$$Tes = T_{6R} + dT_6$$

(24)

It is also possible to reach T_{6S} from T_{6R} through a transformation C (in the base coordinates) which consists of a translation along the x, y and z axes followed by a rotation *0* along an axis k. Thus,

$$T_{6S} = CT_{6R}$$

(25)

where

$$C = Trans(x,y,z)Ro((k,0)$$

(26)

Let n_R, o_R and a_R be the component vectors of the T_{6R} matrix specifying the orientation of the torch at the point R, and n_s, o_s and a< be the corresponding vectors of the T_{6s} matrix. From (24), the corresponding differential vectors (In, do and da arc

$$\dot{d}h \text{ --}i?_s \ -ti\vec{R}$$

(27)

$$\vec{do} = \vec{Os} \text{ ''} \vec{OR}$$

(28)

$$\vec{da} \text{ --}\vec{as} - \vec{a}\wedge$$

(29)

While traveling from point A to point D (in Figure 5), the dTV matrices should be computed to preserve the physical significance of the T_6 matrices at the transition points. Thus, T_{6R} should be computed from c!T_6 according to (24). Geometrically, the loci of the n, o and a vectors of a T_{fi} matrix should be a sphere of unit radius.

Figure 6 depicts the total desired change in each of the n, o and a vectors, while traversing from point A to point D (in Figure 5) in M steps. The components An, Ao and Aa, computed from (30)-(32), arc shown in Figure 6. The arc of the unit circle represents the loci of the n, o and a vectors during the transition. Let $(n_R)_u$, $(o_R)_u$ and $(a_R)_u$ be the unnormalizcd vectors whose tips lie on the point R^7 on the straight line joining points A and D. The subscript u indicates that the vectors arc unnormalizcd. The vectors n_R, o_R and a_R are obtained by normalizing the magnitude of the corresponding vectors to unit length.

The unnormalized vectors of the T_{6S} matrix are computed as

$$(n_s)_u=(n_r)_u+8n$$

(30)

$$(o_s)_u=(o_r)_u+8o$$

(31)

(32)

and then normalized to obtain the n_s, o_s and a_s vectors. **'l'hc** right-hand sides of (27)-(29) are thereby specified completely, and the differential vectors of the dT_6 matrix can be computed to preserve the physical significance of the T'_6 matrix.

Having obtained the (In, do and da vectors of die dT_6 matrix in (15), it remains to compute the dp vector to specify completely the matrix. The vector dp is computed as

$$\vec{dp}=\vec{p}_S-\vec{p}_R$$

where the vectors p_R and p_s arc obtained from (21).

By construction, the $d'lV_6$ matrix satisfies (26). Since the magnitudes of the changes in the joint variables are *not* constrained in the derivation of the $d'l'_6$ matrix, the computed dT_6 matrix satisfies (27). Thus, the $'1\backslash_6$ matrix at the next point S can be obtained by adding the T_6 matrix at the present point R to the computed dT_6 matrix (and consequently there is no need to compute the T_6 matrix at the point S from the updated values of the joint variables when the torch reaches the point S). The real-time computational requirements of this construction arc detailed in Section 5.

4.1. An Iterative Algorithm to Compute the Differential Changes

In applications, such as seam tracing (in which the sample points lie at incremental distances along the scam), tlie required changes in the joint variables may not be incremental. A practical example involves tracing a scam which has large slope variations. The dT_6 matrix is related to the changes in the joint variables through die inverse Jacobian which, in turn, is derived under the assumption of small changes in the joint variables. Many of the scams occurring in practice have slowly varying slopes and application of die inverse Jacobian to make the incremental motions is computationally advantageous. In practice, the scam may exhibit large slope changes at a few points, and the solution obtained (for the differential changes in the joint coordinates to reach the next point) from the inverse Jacobian may exhibit significant errors. The torch is thus placed at the incorrect point on the scam, and a large error (in the position and orientation of the torch) is introduced. To overcome this problem, an iterative algorithm is introduced. A block-diagram of the iterative algorithm is shown in Figure 7.

The algorithm begins at i = 0 with the initialization of the following variables: T_6* (T_6 matrix of the next point), T_{6i} (current T_6 matrix), and q_{i+A} (current values of the joint variables).

'Fhe algorithm implemented at the i-th iteration is ;

$$dT_6 = T_6^* - T_{6i}$$

(33)

$$dQi+i = J"^{1}[dT_{6i},q,_{+}J$$

(34)

$$qi_{+}i = qi-kiq_{i+}i$$

(35)

$$T_6i=F[q_{i+1}]$$

(36)

$$qi=D[qi+i]$$

(37)

where $J"^{1}$ is the inverse Jacobian (in Table 5) for the computation of the differential changes in the joint variables from dT_{6i} and q_{j+J}. (in contrast to the symbolic or numerical inversion of the Jacobian matrix); F denotes the operation of computing the T_6 matrix (in Table 2); and D signifies the computation (delay) time for the forward solution.

Upon substituting (34) into (35),

$$Qi -hi = Qi + J\sim^{1}[dT_{6i},q_{i+1}]$$

(38)

and hence,

$$dq_{i+1} = (q_{i+1} - q_i) = J^{-1}[dT_{6i}, q_{i+1}]$$

(39)

Equation (39), and consequendy the algorithm depicted in Figure 7, is the Ncwton-Raphson method [Atkinson 78] for solving the inverse Jacobian system of nonlinear equations (in Table 5).

The algorithm converges (in theory) when *all* of the components of the dT_{6i} matrix in the block-diagram (in Figure 7) arc zero. In practice, the algorithm is assumed to converge when each of die elements of dl'_{6i} is less than a prc-sct tolerance. The computed vector $<'_i$ contains the desired set-points (in the joint variables) to reach the next position. When the desired changes in the joint variables arc small, the algorithm converges in one iteration and reduces to obtaining the inverse differential solutions from the inverse Jacobian (in Table 5).

For the scams tested with the simulator, the algorithm always converged in a maximum of three iterations (when the preset tolerance was set equal to zero). The computational requirements of the scam tracing algorithm are outlined in the next section.

5. Computational Requirements

The computations required to follow the scam from the present sample point to the next arc outlined in Table 6. The number of iterations required for the transition point computation and iterative algorithm (33)-(37) arc denoted by N_L and N_2, respectively. (For the scams traced by the simulator, typical values are found to be $N_{\{} = 2$ and $N_2 = 1$.) Execution times of the 8087 hardware instructions [Intel 83] are listed in Table 7. These floating point operation times (including the times required to load and store the operand) are used to estimate the time required to move the torch from one sample point to the next. Typical times (shown in Table 6) range from 24 to 29 milliseconds, which correspond to sampling rates of 35-40 Hz. For most welding applications, a sampling frequency of 10 Hz appears to be adequate.

These computational estimates are based upon the *matrix* kinematic modeling of manipulators used throughout this paper. Matrix representations of rotations arc highly redundant. *Quaternions [ftcclcv* 72, Hamilton 69] offer a convenient representation for rotations and can reduce both the storage requirements and computational load [Taylor 79]. The authors estimate that the quaternion implementation of the seam tracking algorithm would increase die achievable sampling rate to 60 Hz.

6. Simulation

To evaluate the algorithm, a software simulator has been developed (in the *C* programming language on a VAX 11/780) for the six degree-of-freedom Cyro robot in our laboratory. The simulation is initialized by retrieving scam data (as coordinates of sample points) from a data file. The first two sampled cross-sections of the seam are used to compute the desired T_6 matrix of the robot at the first point on the mid-seam and to compute the joint position and velocity set-points to reach die desired destination. Upon reaching the first point on the mid-seam, the algorithm computes the coordinates of the transition point on this segment (for the ratio T/T which is entered by the engineer at the start of the simulation) and the total time T required to traverse the next segment. The T_6 matrices at the present and next sample points are used to generate the joint position and velocity set points by the algorithm in (33)-(37). The trajectory from the beginning to end of the transition is computed from (21), and the joint position and velocity set-points arc computed to follow the interpolated curve. Upon reaching the end of the transition, the process is repeated (for each transition point), until the last sample point is reached. The simulation is then terminated and the specified curve is traced.

To achieve a quality weld, die lag or lead angle of the torch must be controlled adaptively. In the case of fillet and lap joints, the torch stand-off must also be controlled. Since an adaptive controller for these parameters remains to be developed, we have included (in our simu-latorXthe facility to specify these control parameters at the beginning of the simulation.

In the software simulator, the torch can be rotated about *two* axes. The first is about an axis *parallel* to the direction of travel and the second is about an axis *perpendicular* to the direction of travel (in the plane of the first axis). This capability allows control over the lead or lag angle of the torch. Facility to specify the stand-off for lap and fillet joints has also been incorporated. The simulator has tracked butt, lap and fillet joints and the experimental results arc highlighted in the next section.

7. Experimental Results

The seam tracking algorithm approximates the curve between sample points by a straight-line. To emphasize the effect of linear interpolation and the choice of sampling distance on the tracking accuracy, the simulator tracked a sinusoidal curve (with uniform spacings of 30 and 10 degrees). The simulation results arc depicted in Figures 8 and 9, respectively. As the sampling distance is *decreased*, the tracked curve approaches the actual curve. The maximum tracking error (which occurs for h = 0.5) is

$$\varepsilon = \frac{3}{16}\Delta C\frac{\tau}{T} - \frac{3}{16}\Delta B$$

and depends upon AB, AC and the ratio T/T. For a particular seam and sample points, AB and AC are constant and the tracking error (with respect to the interpolated curve) is a *linear* function of the ratio T/T. The simulation experiments illustrate that accurate tracking can be achieved by judiciously selecting the sample points and maintaining the ratio (T/T) of transition time to segment time as small as possible.

8. Conclusions

A general-purpose real-time seam tracing algorithm, for implementation on any six degrcc-of-freedom robot, is proposed. The algorithm (which requires knowledge of only one-point-ahead to track a seam) can be applied to a multitude of robotic seam tracking activities such as gluing, surface grinding and flame cutting. The algorithm incorporates the physical interpretation of the T_6 and dT_6 matrices to realize scam tracking. To reduce the computational requirements, the paper introduces the concept of a modified dT_6 matrix. The inverse Jacobian solution is generalized (according to Newton's method) to compute both large and small changes in the joint coordinates.

To test the efficacy of die proposed seam tracing algorithm, a simulator has been written and tested on a VAX 11/780. The simulation results arc highlighted in Section 7 of [Khosla 83]. The tracking accuracy is a function of the sampling distance because of the straight-line approximation between two successive sample points, and the tracking error increases with the increase in ratio of the transition time to the segment travel time.

Future activity will focus on die adaptive control of the weld parameters and dynamic robot control. Successful practical implementation will depend upon the availability of faster processors and the experimental performance evaluation of the algorithm.

References

[Agin 821 G. J. Agin and P.T. I lighnam.
A Movable Light Stripe Sensor for Obtaining Three Dimensional Coordinate Measurmcnts.
In *Proceedings ofSPIE: The Society ofOptical Engineers 360,* pages 326-333. San Diego, CA, August 21-27, 1982.

[Atkinson 78] K. R. Atkinson.
An Introduction to Numerical Analysis.
John Wiley and Sons, New York, 1978.

[Bccler72] M. Heeler, R. W. Gosper and R. Schrocppel.
"Hakmem".
Al Memo 239, Artificial Intelligence Laboratory, Massachusetts Institute of Technology, Cambridge, MA 02139, February, 1972.

[Bollingcf71] J. G. Bollingcr and II. L. Harrison.
Automated Welding Using Spacial Seam Tracings.
Welding Journal 50:787-792, November, 1971.

[Dcnavit 55] J. Dcnavit and R. S. Hartenberg.
A Kinematic Notation for Lower Pair Mechanisms Based on Matrices.
*Journal of Applied Mechanics 11*r:215-221, June, 1955.

[Hamilton 69] W. R. Hamilton.
ElementsofQuaternions.
Chelsea Publishing Company, New York, 1969.

[Hill 80] J. W. Hill J. Krcmers and D. Nit/an.
Advanced Automation for Ship Building.
Final Report, Department of Navy Contract N00024-80-C-2026, SRI International, Menlo Park, CA 94025, November, 1980.

[Intel 83] *iAPX86/88, 186/188 User's Manual Hardware Reference*
Intel Corporation, 3065 Bowers Avenue, Santa Clara, CA 95051,1983.

[Khosla 83] P. K. Khosla.
Simulation of a Sensor Based Robotic Spatial Seam Tracing System.
Master's thesis, Department of Hlcctrical and Computer Engineering, Carncgic-Mcllon University, Pittsburgh, PA 15213, 1983.

[Masaki 79] I. Masaki.
Kawasaki Pais Memo No. 7904, Pais Center, Robot Group.
Technical Report, Kawasaki Heavy Industries Ltd., Japan, April, 1979.

[Masaki 81] I. Masaki, et al.
Arc Welding Robot with Vision.
In *PUeventh International Symposium on Industrial Robots*, pages 813-817. Tokyo, Japan, October 7-9, 1981.

[Paul 81] R. P. Paul.
Robot Manipulators: Mathematics, Programming and Control.
MIT Press, Cambridge, MA, 1981.

[Taylor 79] R.H.Taylor.
Planning and Execution of Straight Line Manipulator Trajectories.
IBM Journal ofResearch and Development 23(4):424-436, July, 1979.

[Tomi/uka 80] M. Tomizuka, D. Dornfcld and M. Porccll.
Application of Microcomputers to Automatic Weld Quality Control.
Journal ofDynamic Systems, Measurement, and Control 102(2):62-68, June, 1980.

[Whitney 72] D. F, Whitney.
The Mathematics of Coordinated Control of Prosthetic Arms and Manipulators.
Journal ofDynamic Systems, Measurement, and Control 94(4): 303-309, December, 1972.

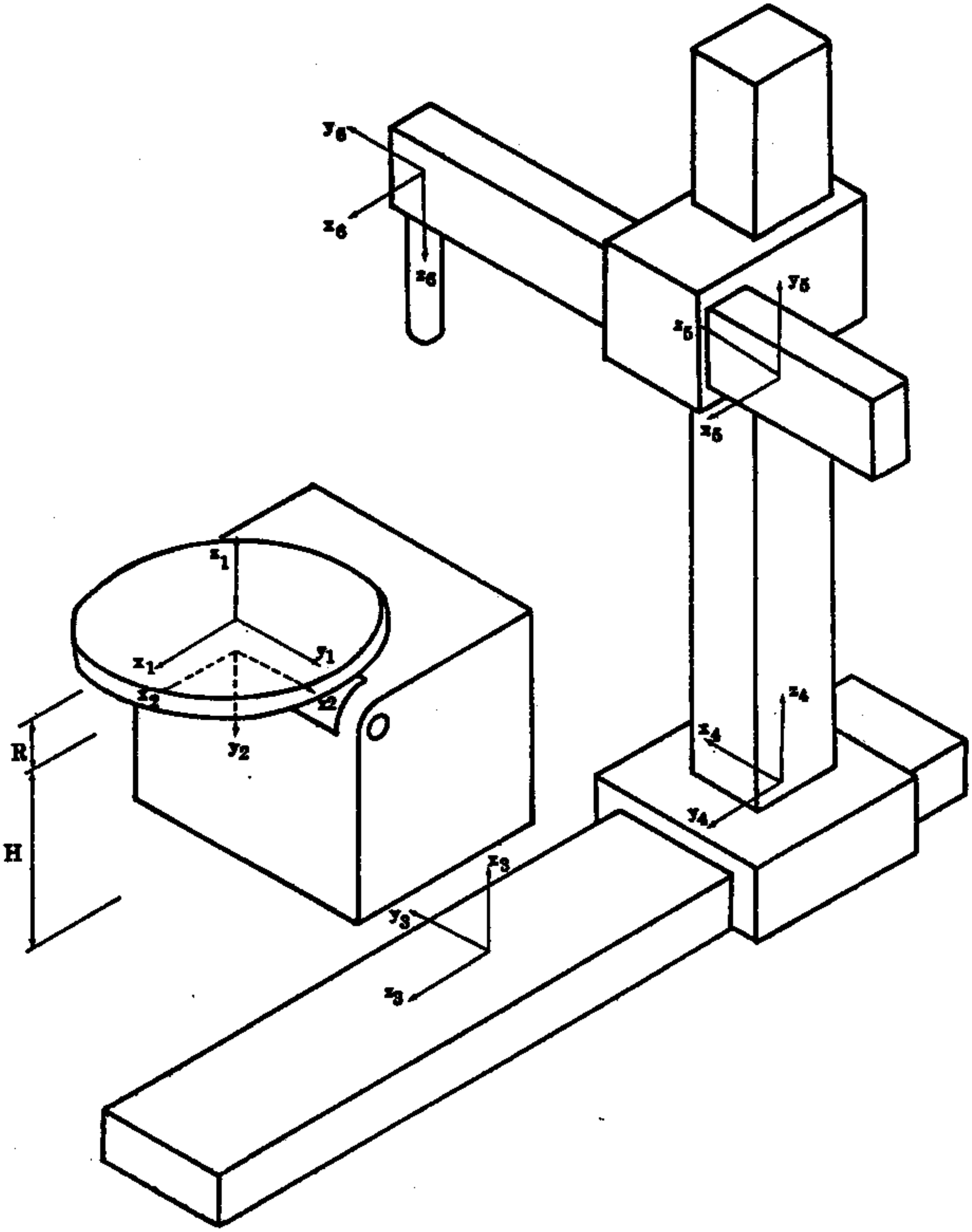

Figure 1: Link Coordinate Frames of the CYRO Robot

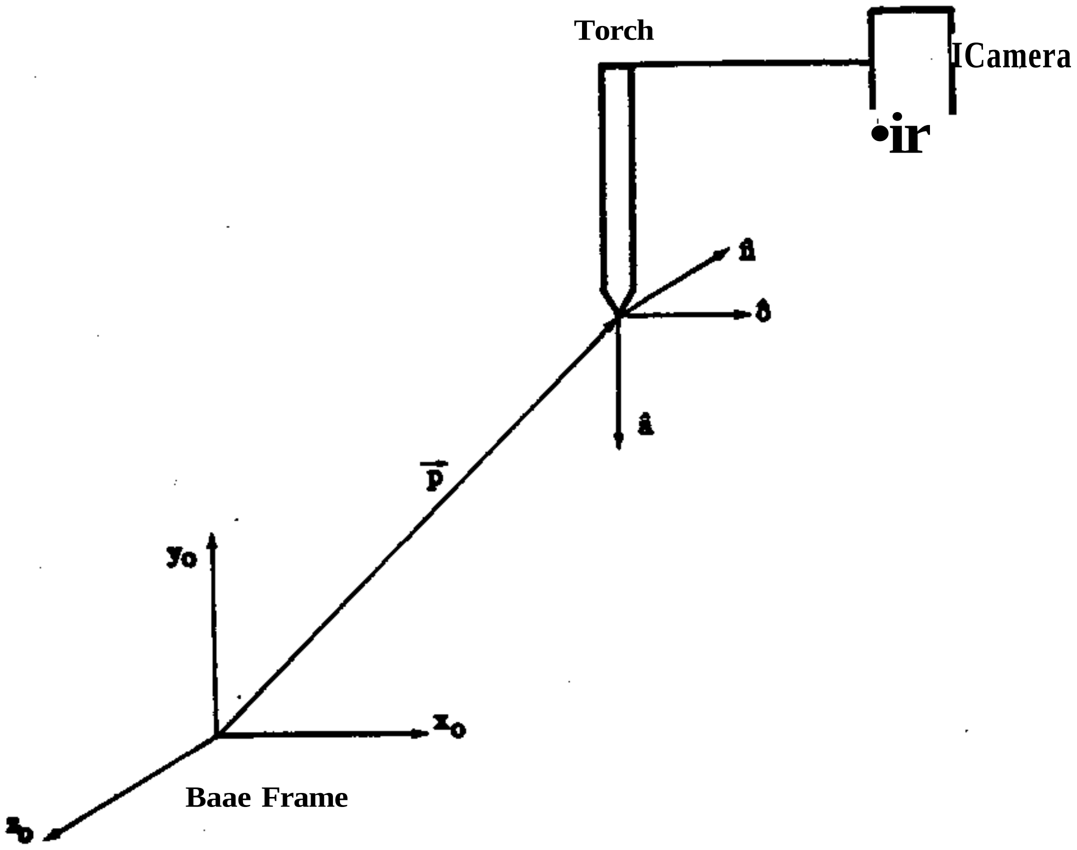

Figure 2: Physical Interpretation of the T_6 Matrix

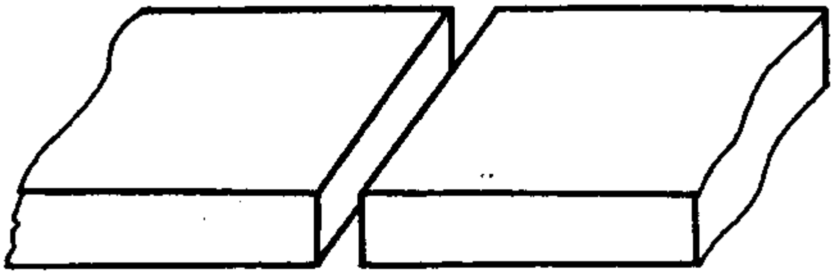

Figure 3: Butt Joint

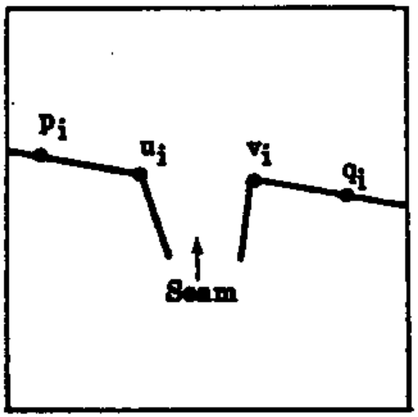

Figure 4: Camera Image of a Butt Joint

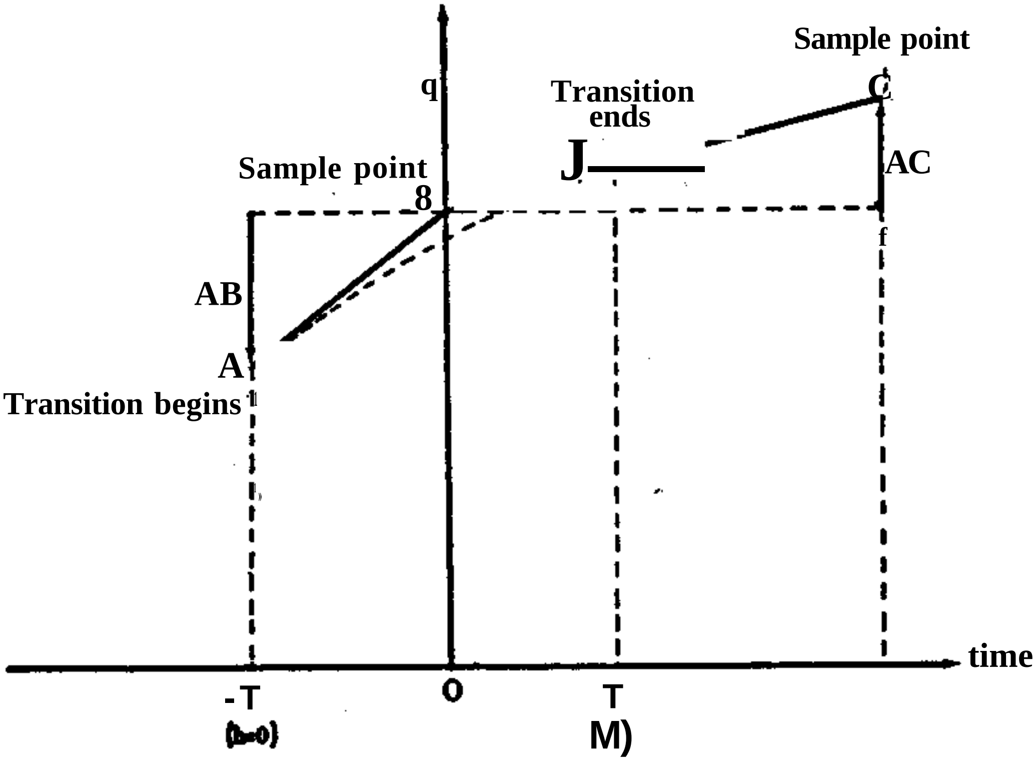

FigureS: A Transition Segment

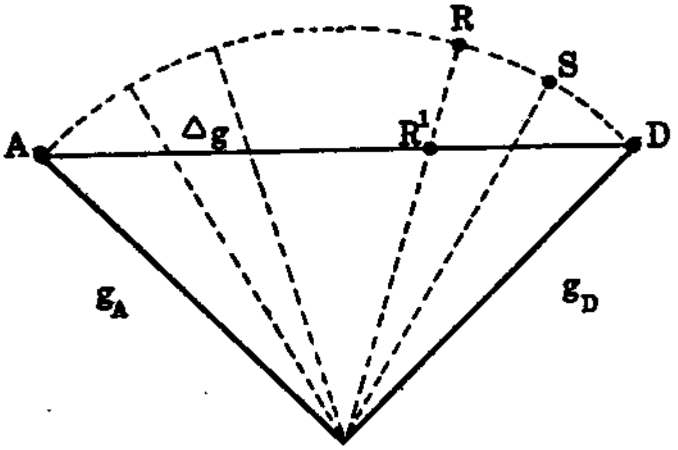

Note* **The generic vector g symbolizes the normal (n), orientation (o) and approach (a) vectors.**

Figure 6: Locii of n, **o** and a Vectors

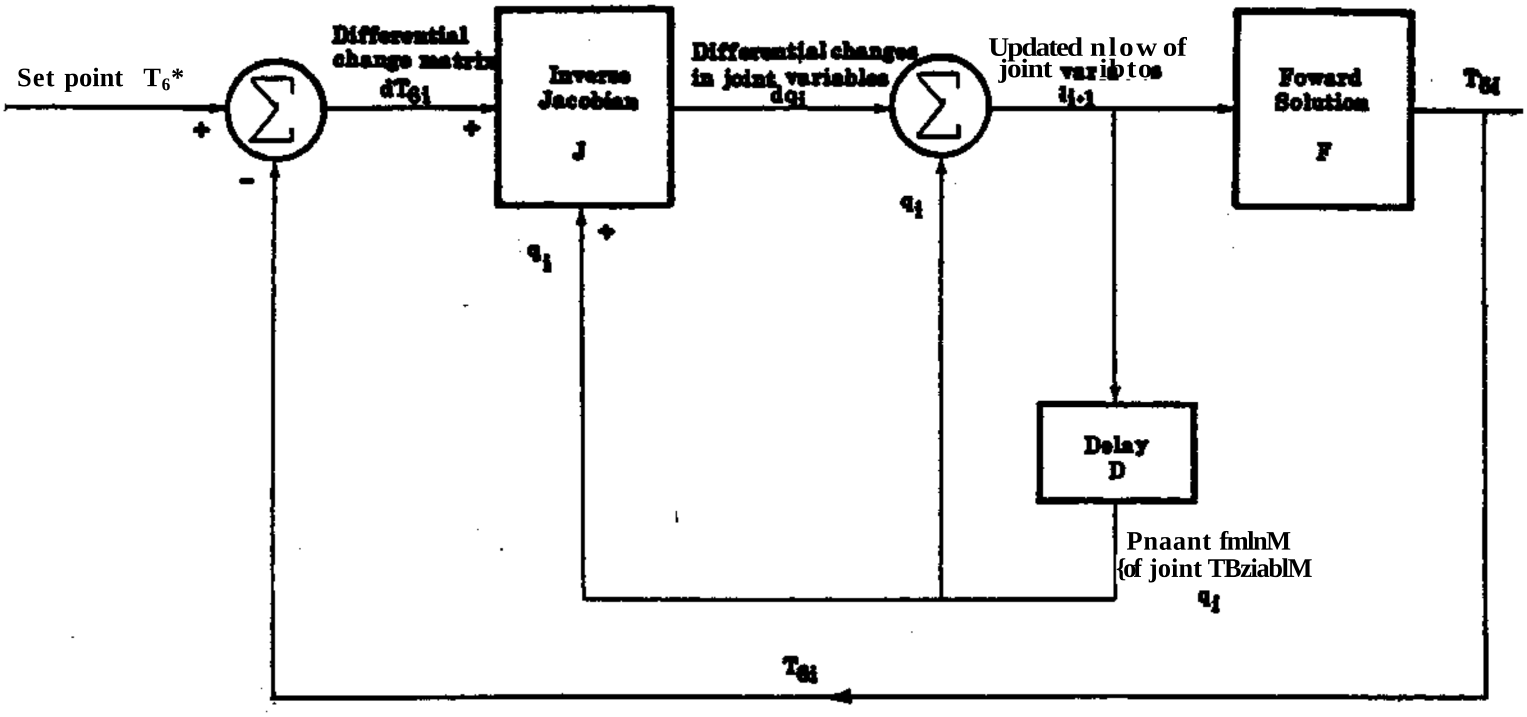

Figure 7: Block Diagram of the Iterative Algorithm

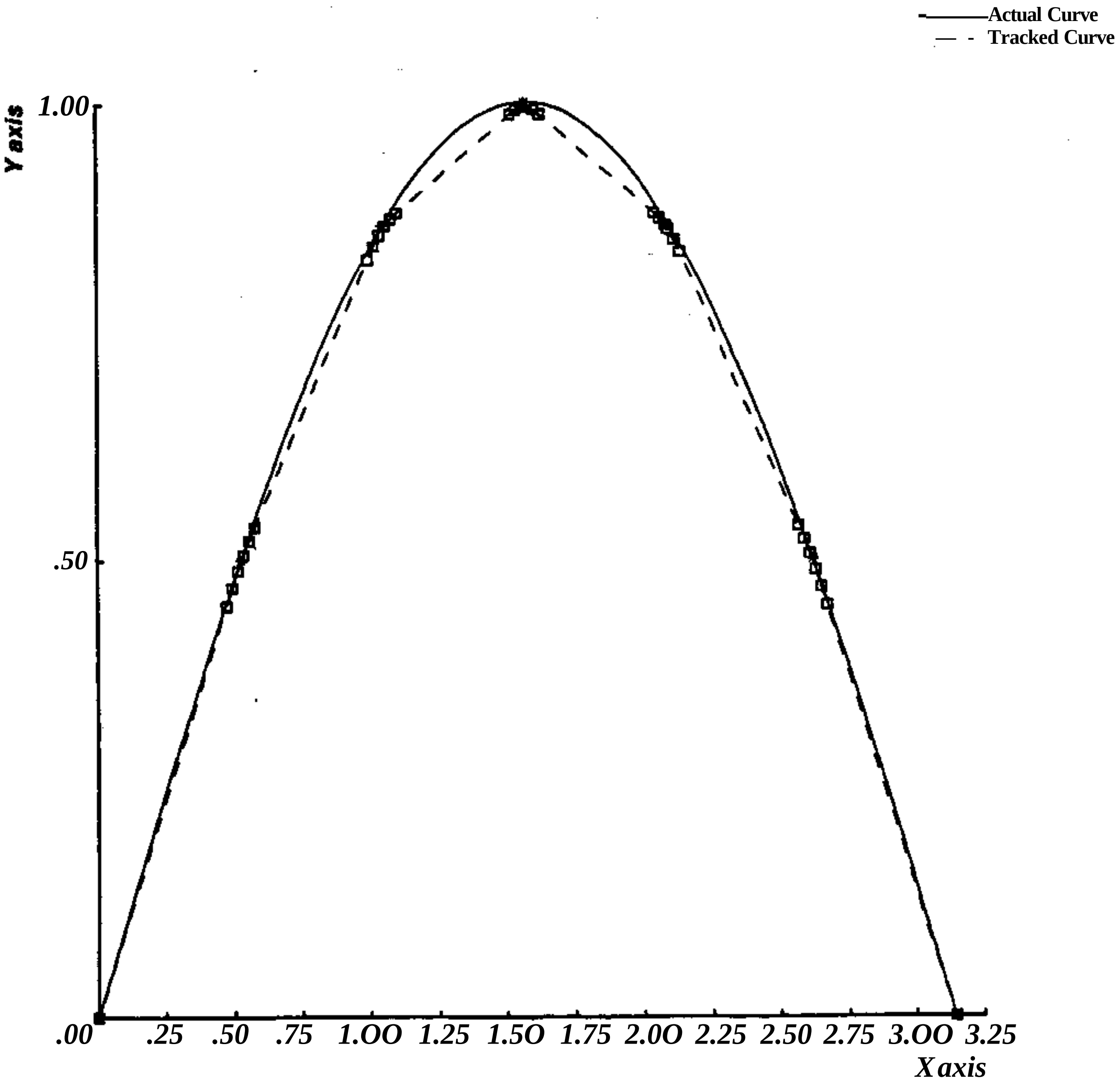

Figure 8: Sinusoidal Seam Tracking (30 degrees sampling interval)

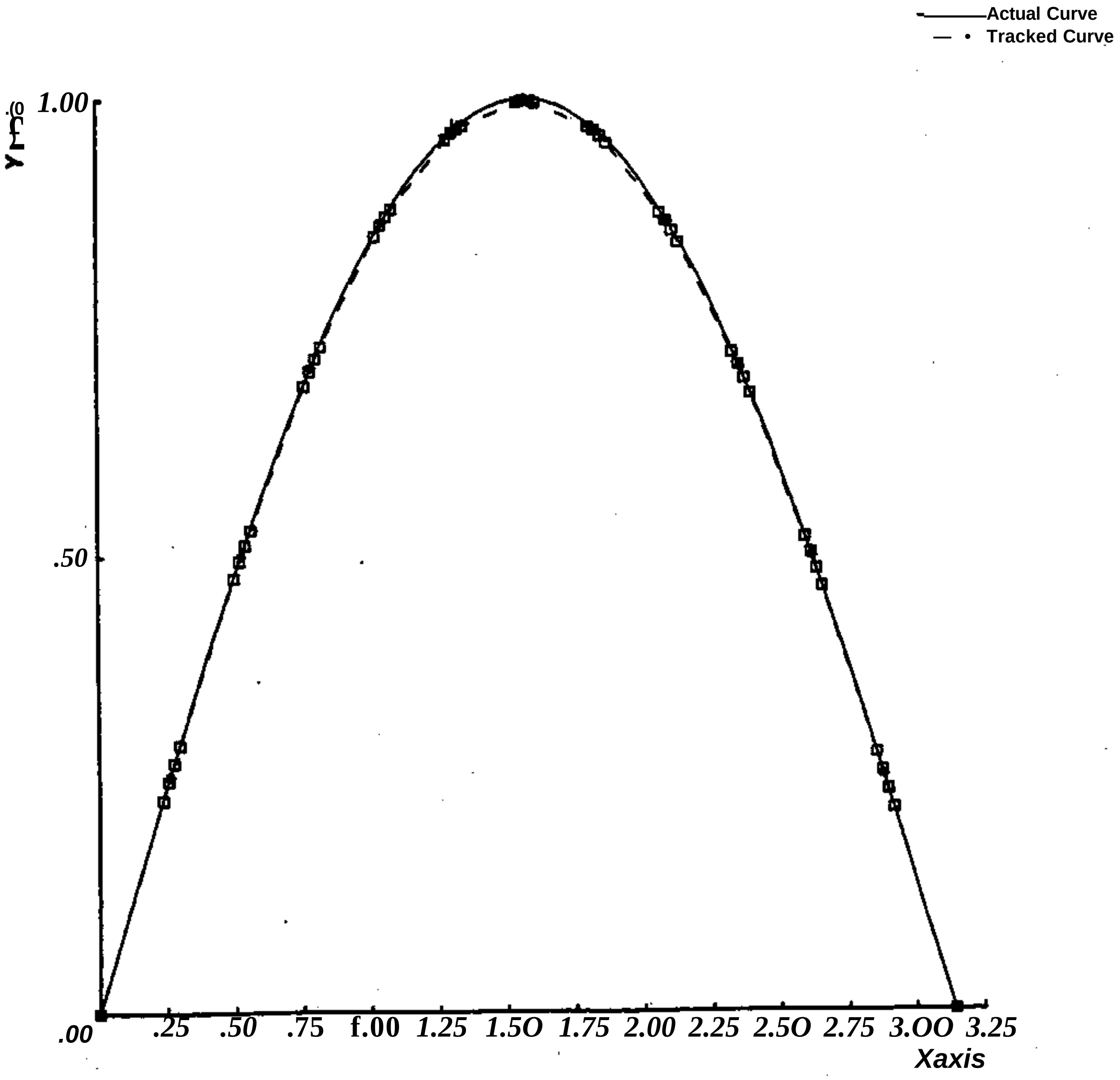

Figure* Sinusoidal Seam Tracking (10 degrees sampling interval)

Link	Variable	8	a	a	d
1	θ_1	θ_1	-90	0	-R.
2	θ_2	0_2-9O	-90	-H	L
3	*3	90	90	0	*3
4	*24*	90	90	0	*4
5	*ys*	0	0	0	*y%*
6	ft	ft	0	0	0

Definition of the Parameters

8 is the angle ofrotation about the raxis

a is the angle ofrotation about the x-axis

a is the length oftranslation along the x-axis

d is the length oftranslation along the z-axis

Table 1: Link Parameters of the CYRO Robot

$$
{}^{0}T_{6}=\begin{bmatrix}
C_1C_2C_6+S_1S_6 & -CAS6+S_1C_6 & -C_1S_2 & C_1(z_4S_2 +X3Q -HSj) -Si(-y_5 +L) \\
S_1C_2C_6-C_1S_6 & -S_1C_2S_6-C_1C_6 & -S_1S_2 & 82(2482 +X3C2 -HSj)+Ci(-y_5 +L) \\
-S_2C_6 & S_2S_6 & -C_2 & (24C2-X_3S_2-HC2) -R \\
0 & 0 & 0 & 1
\end{bmatrix}
$$

Table 2: Forward Solution of die CYRO Robot

Joint coordinate	Analytical Expression	Conditions
θ_1	$atan2\left(\frac{a_y}{a_x}\right)$	7-$_6$(2,3)> 0
θ_1	*alanl* $\left(\frac{-q\ \text{—Z-}}{-a_x}\right)$	**r$_6$(2,3)< 0**
0i	*atanl* $\left(\frac{\text{-}ic_{iax} \quad +s_{iay}))]}{(\text{-«,})}\right.$ **j**	
x_3	$C_1C_2p_x + S_1C_2p_y - S_2p_z - S_2R$	
2A	*C"'Z?-ZT*$^{R+H}$	
y_5		
*	*atanl* $\left(\frac{o_z}{-n_z}\right)$	*8$_2$>* **0**
*	*atanl* $\left(\frac{o_z}{-n_z}\right)$ **+ 180°**	^< . 0

NOMENCLATURE

C; **is** ***the Cosine of the i-th joint angle***

Si is the Sine of the irth joint angle

atan2 is the double argument arc tangent junction

Table 3: Reverse Kinematic Solution of the CYRO Robot

$$\frac{\partial T_6}{\partial \theta_1} = \begin{bmatrix} \text{-<CiC}_2\text{C« +SiSt)(var]) +(SiC}_2\text{C6 - }C_1S_6\text{)(var2)} \\ \text{-(C}\cdot_x\text{Ci\% +SAH>}^{arl}\text{> +("SiQS6 -QC6)(var2)} \\ \text{QS\^{}varl) -SjS}_2\text{(var2)} \\ -S_2C_6 \\ S_2S_6 \\ -C, \end{bmatrix}$$

$$\frac{3T«}{\partial \theta_2} = \begin{bmatrix} \text{-C}_2\text{Q(var3) +S}_2\text{Q(var4)} \\ \text{C|S|(var3) -SA<(var4)} \\ \text{SjCvari) -Cj(var4)} \\ -S_6 \\ -Q \\ 0 \end{bmatrix}$$

$$\frac{3]\wedge}{3*3} = \begin{bmatrix} C_6 \\ -S_6 \\ 0 \\ 0 \\ 0 \\ 0 \end{bmatrix} \qquad \frac{\partial T_6}{3*4} = \begin{bmatrix} 0 \\ 0 \\ -1 \\ 0 \\ 0 \\ 0 \end{bmatrix}$$

$$\frac{3T_6}{\partial y_5} = \begin{bmatrix} §6 \\ Q \\ 0 \\ 0 \\ 0 \\ 0 \end{bmatrix} \qquad \frac{HL}{30_6} = \begin{bmatrix} 0 \\ 0 \\ 0 \\ 0 \\ 0 \\ 1 \end{bmatrix}$$

NOMENCLATURE

varl =Si(z4Sj +x$_3$C$_2$ -HSj) +Q(-y$_5$ +L)

var2 sC$_1$(z$_4$S$_J$ +x$_3$Cj -HS2) +Si(-y$_3$ +L)

var3 =s - 24Q + X3S2 + HCj

var3 ^*uSj* +XjQ -HSj

TaMt4: Column Vectors of theJacobian matrix

DIFFERENTIAL JOINT COORDINATES

$$d\theta_1 = \frac{(-S_1da_x + C_1da_y)}{(C_1a_x + S_1a_y)}$$

$$d^{-} = \frac{NC_2d(NS_2) - NS_2d(NC_2)}{(NSJ^2 + (NC_2)^2}$$

*

$$dz_4 = C_2A_xd0_2 + S_2A_2 + C_2dp_z - S_2A_3d\theta_2$$

$$dy_5 = Cip_xd\$i + S\backslash dp_x + Sip_yd8i - C\backslash dp_y$$

$$d\theta_6 = \frac{C_6do_z + S_6dn_z}{S_6o_z - C_6n_z}$$

NOMENCLATURE

$$NC_2 = -a_t$$

$$d(NC_{2)} = -da_t$$

NS2 = """"Cltx — •S'l^y

$$d(NS_{2)} = S\backslash Q_xd0\backslash - C\backslash d(i_x - C\backslash ciyCi\$x - S\backslash da_y$$

$$A\backslash = C\backslash p_x + S\backslash Py$$

$$A_2 = {\sim}{\sim}Slp_Xd\$l + C\backslash dp_x + C\backslash Pydth+Sidpy$$

Table 5: Inverse Jacobian ofthe CYRO Robot

STEP	*	-h	÷	√	SIN/ /cos	TIMHin millisec
Find the mid-scam						
Butt Joint (1)		'3	3			0.384
Lap/Fillet Joint (2)	3	6				0.462
Compute segment travel time T						
Butt Joint	23	39	I	5		3.611
Lap/Fillet Joint	32	61	1	6		5.256
Find transition point						
Butt Joint	23*N i	39*N,	**Nt**	5*N ,		7.222
Lap/Fillet Joint	$32*N_t$	6l*Ni	**Ni**	$6*N_V$		10.512
Computation of						
a Vector	9	14	5	1		1.611
o Vector (6)-(7)	15	11	3	1		1.675
n Vector (8)	3	6				0.462
Compute dT $_6$ Matrix		12				0.576
Normalization	9	4	3	3		1.125
Iterative algorithm (33) - (37)	$66*N_2$	$54*N_2$			$6*N_2$	7.206
'Total						
Butt Joint	62 + 23*Nt + $66*N_2$	86 + 39*N, + $54*N_2$	15 + N,	**10 + Nj**	$6*N_2$	23.872
Lap/Fillet Joint	73+23*Ni + $66*N_?$	108 + 39*Ni + $54*N_2$	15 + N,	10 + N,	$6*N_2$	28.885

Table 6: Computational Requirements of the Scam Tracing Algorithm

Function	Time(jis)
Multiply	27
Add	17
Divide	39
Square Root	36
Tangent	90
Exponentiation	100
Load	10
Store	21

Table 7: Execution Times of the 8086/8087 Microprocessor^ MHz Clock) [Intel 83]